Understanding the Hepatic Disposition of Statins to Improve Predictions of Safety and Efficacy

Teresa Heslop
GLAXOSMITHKLINE

Teresa Louise Heslop (Teresa.l.Heslop@GSK.com)

GSK Supervisor: Dr Kunal Taskar,

University of Strathclyde Supervisors:

Professor Helen Mary Gant, Professor Simon MacKay

Table of Contents

ABSTRACT

To date, little is known about the hepatic transport of statins by the multi resistance proteins MRP2, MRP3 and MRP4 or their inhibitory potential against these same carrier proteins. By inference, the potential clinical consequences of statin transport and inhibition are not fully characterised.

This thesis examines seven statins, their transport properties against MRP2, MRP3 and MRP4 and their ability to act as transport inhibitors. The inside-out vesicular model was employed where only a single MRP transporter was transfected. Key findings were;

Statins identified as substrates:

MRP2: Rosuvastatin

MRP3: Pravastatin, rosuvastatin

MRP4: Fluvastatin, pitavastatin, pravastatin

Statins identified as inhibitors:

MRP2: All statins (weak inhibitors except for lovastatin)

MRP3: All statins moderate to strong inhibitors especially atorvastatin

MRP4: All moderate inhibitors except pravastatin (weak)

Notably, our findings imply that statins acting as perpetrators of MRP3 and MRP4 inhibition may be of more clinical relevance than their behaviour as substrates.

.

1 INTRODUCTION

1.1 Aim

The aim of this project was to contribute to the understanding of the hepatic disposition of statins with respect to the Multi-Resistant Proteins MRP2, MRP3 and MRP4 with a view to improving predictions of statin safety and efficacy. The disposition of statins has previously been explored with respect to MRP2, but to date there has not been a thorough investigation into the possible contribution of MRP3 and MRP4. In this thesis several areas will be discussed in relation to the aim. These will include an overview of statins, focusing on their use, disposition, and implications of drug-drug interactions; an overview of hepatic transporters with attention on MRP2, MRP3 and MRP4; and review of *in vitro* models to study drug transport and the associated supporting analytical techniques.

1.2 Statins

According to the World Health Organisation, ischemic cardiovascular disease (CVD) is the major cause of mortality [1]. Most frequently, CVD results from atherosclerosis, a disease where plaque (white blood cells and cholesterol containing LDL - Low Density Lipoprotein) accumulates within the walls of arteries, eventually resisting the flow of blood [2] . Hypercholesterolemia (high levels of circulating cholesterol) is implicated in atherosclerotic disease [3, 4]. Cholesterol is synthesised in mammalian cells from acetyl coenzyme A *via* a multi-stage process involving the reductase enzyme, 3-hydroxy-3-methylglutaryl coenzyme A (HMG-CoA). By inhibiting HMG-CoA, levels of circulating cholesterol are reduced (Figure 1.1). HMG-CoA reductase inhibitors, commonly referred to as statins, are a class of compounds that inhibit the production of cholesterol in the liver and are used extensively for the treatment of hypercholesterolemia [5-7].

Figure 1.1 Schematic for the synthesis of cholesterol in the liver and the inhibition of this process by statins.

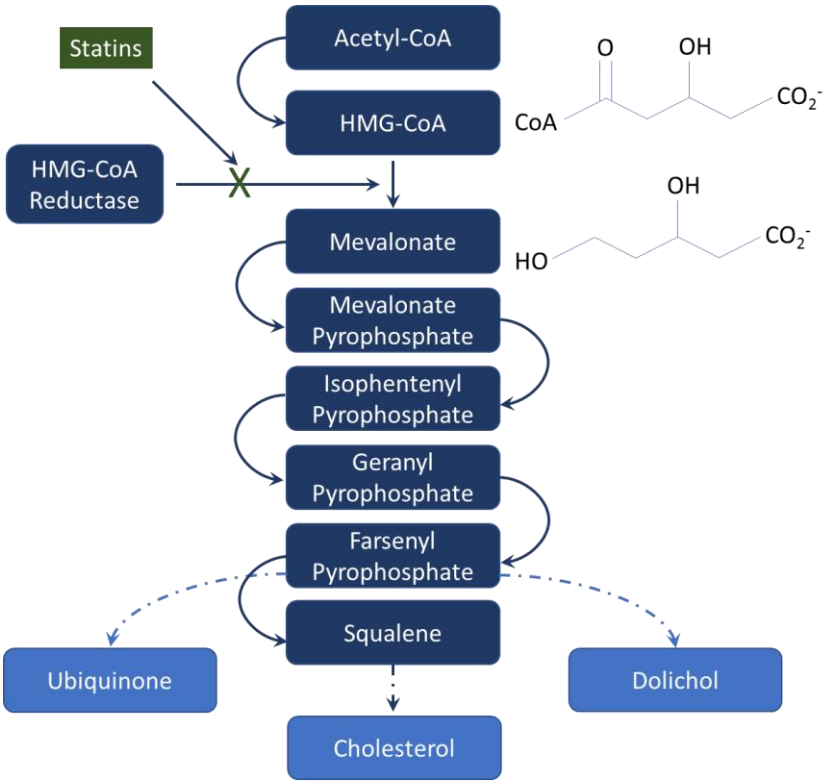

The basic structure of all statins is shown in Figure 1.2 with the common moiety being the hydroxyglutaric group, which structurally resembles HMGCoA. The various statin drugs differ through the substituted ring structure and their substituents appended to this hydroxyglutarate. The physicochemical properties of the statins are shown in Table 1.

Figure 1.2 Hydroxyl glutaric group, pharmacophore of all statins

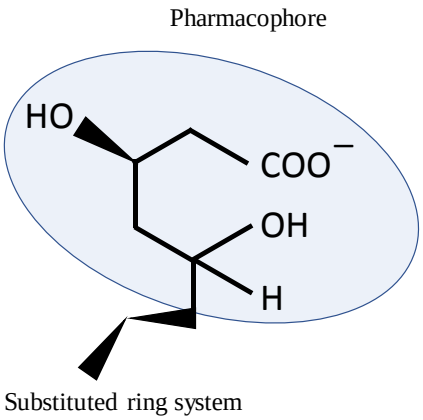

Table 1: Structure of Statins (acid forms only) and Basic Physicochemical Properties

Statin	Structure	MW	Pka[1]	[1]LogP	[2]LogD [7.4]
Cerivastatin	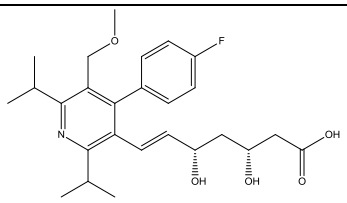	459.55	4.24	3.18	1.66
Fluvastatin	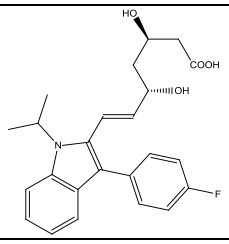	411.47	4.27	4.57	1.34
Lovastatin	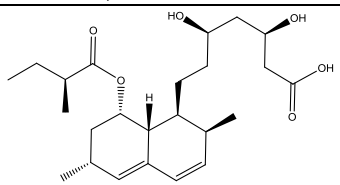	422.27	4.31	4.12	1.04
Atorvastatin	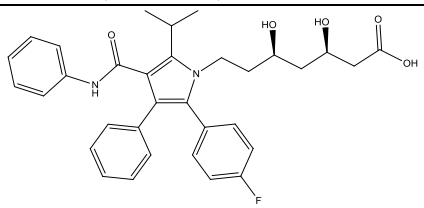	558.64	4.29	3.85	1.81
Pitavastatin	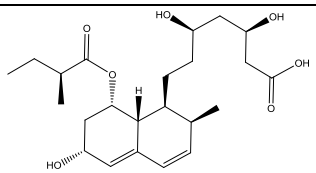	421.46	4.24	1.92	-1.2
Simvastatin	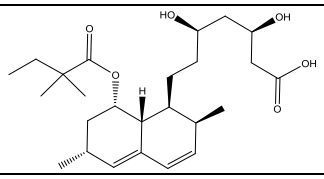	436.28	4.31	4.54	1.45
Rosuvastatin	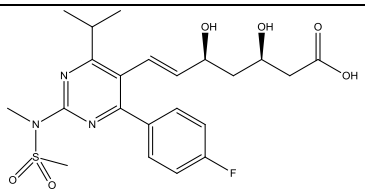	481.5	4.25	0.89	-0.24
Pravastatin	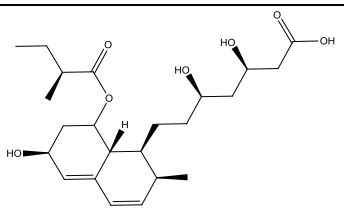	424.5	4.31	2.21	-0.88

[1] data from chEMBL www.ebi.ac.uk, [2] data from [8, 9],

Between 2016-2017, simvastatin and atorvastatin were reported to be the top 10 prescribed drugs in the UK, with a combined estimated 60 million items dispensed in the year [10]. In 2014 the UK National Centre for Clinical Excellence (NICE) [11] published guidelines recommending that statins should be offered to people with a 10% risk or greater of developing CVD [12].

Statins are generally well tolerated and are characterised by a good overall safety profile [13] however, adverse muscular effects (myopathy) have been associated with their use, ranging from mild muscle pain through to rare and possibly fatal rhabdomyolysis (0.3-13.5 cases of per 1000000 statin prescriptions) [14-16]. Rhabdomyolysis is the breakdown of muscle tissue, symptoms include muscle pains, weakness in the muscles, vomiting and confusion. Other causes of rhabdomyolysis are through muscle injury i.e strenuous exercise. It is believed that the interruption of the HMG-CoA biosynthetic pathway causes depletion of downstream metabolites, which are important in balancing intracellular signalling leading to cell death. The occurrence of muscle complaints appears to be dose related and with the more lipophilic statins i.e simvastatin. Rhabdomyolysis is most noted in patients prescribed satins where a concomitant medication has inadvertently inhibited CYP3A4 [17]. It was previously assumed that rhabdomyolysis was only associated with lipophilic statins which can passively diffuse in to the muscle, but as statins have a range of lipophilicities (from lipophilic lactone prodrugs such as simvastatin, to more polar compounds such as rosuvastatin) there is at present no clinical evidence relating the level of lipophilicity of a statin and its potential to cause myopathy. A class effect or associated structure-activity relationship (SAR) therefore appears unlikely [18]. Notably, it is known that alongside OATP2B1, MRP1, MRP4 and MRP4 transporters are also expressed in the sarcolemma of human skeletal muscles [19, 20], which could have implications for statin disposition in this tissue type.

1.3 Metabolism and Disposition of Statins

The metabolism and disposition of statins is summarised in Table 1.1 with the key hepatic transporters shown in Figure 1.3. Metabolism has been widely studied with respect to CYP-mediated metabolism [18, 21, 22], and disposition with regards to the hepatic organic anion-transporting polypeptides (OATPS)[23, 24] and sodium/taurocholate co-transporting peptide (NTCP) [25]. The majority of CYP substrates are typically lipophilic [26], therefore the more lipophilic statins such as simvastatin, lovastatin and atorvastatin are extensively metabolised by CYP3A or CYP2C9 in the liver [27, 28]. Transporters are crucial in the uptake of statins into the liver as this the major site of their action[29]. OATP has a significant role, particularly OATP1B1 and OATP1B3. OATP mediated uptake has a greater impact on the systemic exposure of the statins compared with metabolic clearance. Canalicular efflux *via* the multidrug resistance protein-2 transporter (MRP2) and Breast Cancer Resistance Protein (BCRP) have also been shown to play a role in the biliary excretion of rosuvastatin. [30-32]. Recent work has also recognised that the basolateral efflux transporter MRP4 may play a role in the disposition of rosuvastatin [33, 34]. Whereas rosuvastatin has received the greatest attention with respect to interactions with MRP2, the impact of MRP transporters on the disposition of other key statins is still in its infancy [35].

Figure 1:3 Schematic of key hepatic enzymes and transporters involved in the disposition of statins.

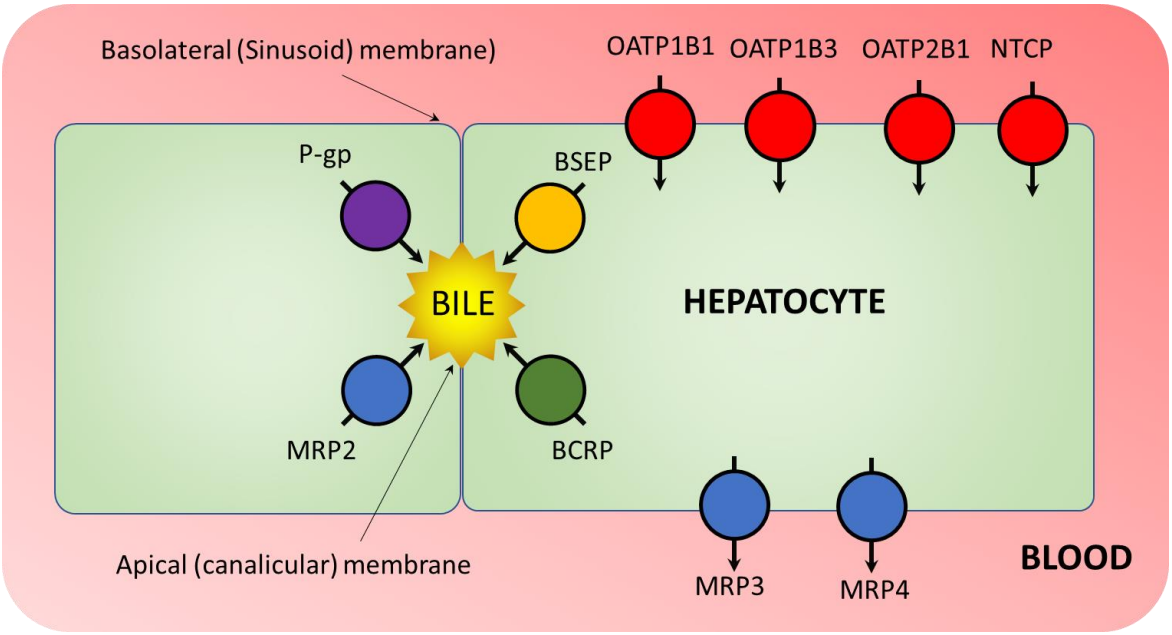

Pg-p: P-glycoprotein (also known as MRD1)

Table 1:2 Key Enzymes and Transporters Involved in the Hepatic Metabolism, Uptake and Efflux of Statins

Statin	Enzyme(s) involved in metabolism	Major transporters involved in disposition	Routes of elimination (listed in order of significance)
Atorvastatin	**CYP3A4**	Uptake**: OATP1B1,** OATP1B3, OATP1A2, NTCP, Efflux**: BCRP**, MRP2, P-gp	Metabolism
Cerivastatin (withdrawn)	CYP2C8 CYP3A4	BCRP and OATP1B1	Metabolism
Fluvastatin	**CYP2C9** CYP2C8 CYP3A4	**BCRP**, OATP1B1, **OATP1B3** and OATP2B1	Metabolism
Lovastatin	CYP3A4 CYP2C9	**OATP1B1** and P-gp	Metabolism
Pitavastatin	CYP3A4 CYP2C9	BCRP, MRP2, NTCP, OATP1B1, **OATP1B3** and P-gp	Biliary clearance
Pravastatin	Non-CYP	**OATP1B1,** MRP2, NTCP, OATP1B3, OATP2B1, P-gp (OAT3 renal)	Non-CYP metabolism Renal clearance
Rosuvastatin	CYP2C9	**BCRP**, MRP2, **NTCP**, OATP1A2, **OATP1B1**, OATP1B3, OATP2B1, P-gp (OAT3 renal)	Biliary clearance Renal clearance
Simvastatin	**CYP3A4** UGT1A1 UGT1A3	**OATP1B1**	Metabolism Biliary clearance

[1]Shitara and Sugiyama (2006). Table adapted from Chatzizisi (2010). Major transporters and enzymes are highlighted in bold.

1.4 Review of MRP2, MRP3 and MRP4[36]

MRP2, MRP3 and MRP4 are localised either apically or basolateral across cells in various tissues, such lungs, liver, intestine, kidneys. In this thesis, the focus is primarily on the liver.

1.4.1 Overview

The Multidrug Resistance Proteins MRP2, MRP3 and MRP4 (also known as ABCC2, ABCC3 and ABCC4) are from the ATP-binding cassette (ABC) family of transporters. They are able to transport a diverse range of lipophilic anions such as bile acids, glucuronide and sulphate conjugates [37-42] and are especially recognised for imparting resistance to anti-cancer drugs [43, 44] (Table 1.3).

Structurally, the active site of MRP transporters consists of two nucleotide-binding domains (NDB) and two transmembrane domains (TMD) (Figure 1.4). Transport across these domains is driven by energy gained from the hydrolysis of adenosine triphosphate (ATP) to adenosine diphosphate (ADP), by the ATPase subunit of the transporter. Depending on the length of the surrounding membrane spanning domains (MSD), MRPs are classified into either ’large’ or ’short’. MRP2 and MRP3 have three MSDs and are deemed to be large, whereas MRP4, with only two MSDs is categorised as short [45, 46]. The key structural features of these MRPs are shown in figure 1.4

1.4.2 Localisation and Functions

MRP2 is expressed at the bile canalicular membrane and assists in the biliary efflux of bile acids [47]. A defect in MRP2 is associated with Dubin-Johnson syndrome, characterised by a yellowing of the skin because of conjugated hyperbilirubinemia [48, 49].

MRP3 is an efflux transporter localised on the basolateral cell membrane of hepatocytes, where it is involved in the regulation of bile acids and transports similar substrates to MRP2.

This may account for the upregulation of MRP3 as a protective mechanism in the case of cholestasis where the bile canalicular ducts become blocked. [50].

Figure 1.4 Structural features of the Multi Resistance Proteins MRP2, MRP3 and MRP4.

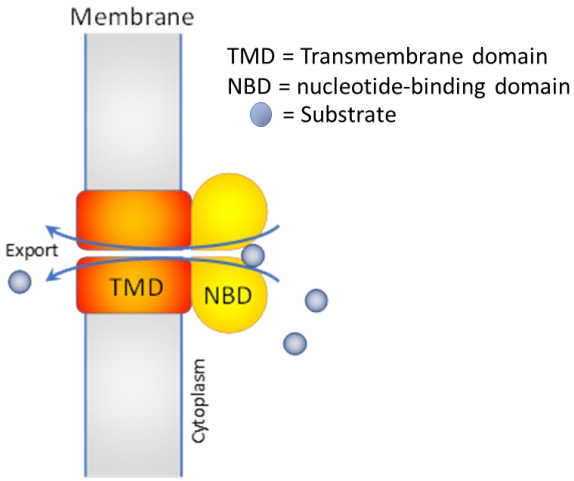

MRP4 is also expressed on the basolateral cell membrane, although at much lower levels than MRP3. Although its substrate specificity is similar to MRP2 and MRP3, MRP4 also mediates the transport of cyclic nucleotides [51] in other tissues such as the intestine and blood brain barrier. Up-regulation of MRP4 is also observed in cholestatic conditions as another back up system for the removal of bile acids [52]

Table 1.3 Key substrates and inhibitors for Multi Resistance Proteins MRP2, MRP3 and MRP4 (Derived from SOLVO Biotechnology knowledge centre)

Transporter	Example Substrates	Example Inhibitors
MRP2 (ABCC2)	Glutathione and glucuronides e.g LTC_4, $E_2$17βg, Bilirubin and its conjugates Dianionic bile salts Methotrexate, etoposide, olmesartan, mitoxantrone, glucuronidated SN-38	Cyclosporine, Delavirdine Efvienz Benzbromarone Probenecid
MRP3 (ABCC3)	Glutathione and glucuronides e.g LTC_4, $E_2$17βg, bilirubin glucuronide Bile salts e.g. taurocholate, glycocholate Methotrexate, fexofenadine Morphine-6-glucuronide Morphine-3-glucuronide	Delavirdine Efvienz Benzbromarone Probenecid MK751
MRP4 (ABCC4)	Conjugated steroids e.g $E_2$17βg, DHEAS Prostanoid e.g. PGE Cyclic nucleotides e.g. cAMP, cGMP Bile salts e.g. cholate, taurocholate, glycocholate Antivirals, methotrexate, topotecan	Celecoxib Diclofenac MK571 probenecid

1.5 Drug Drug Interactions (DDI)

Whenever two or more drugs are taken together, there is the possibility that one drug could affect the pharmacokinetics of the co-administered agents or their associated metabolites. For the pharmaceutical industry, understanding and predicting drug-drug interaction (DDI) potential is of high importance because altered drug PK could result in significant clinical consequences [53]. These may include;

i) Decrease in the exposure of a drug, leading to reduced efficacy that could then require a dose adjustment.

ii) Elevation in the exposure of a drug or its metabolite, leading to undesirable effects i.e. rashes, QT prolongation or Torsades de Pointes (TdP) arrhythmias. These could result in safety concerns/contraindications and therefore labelling restrictions.

iii) Therapeutic monitoring, where the patient is required to attend additional assessments i.e blood tests, to ensure that the drug therapeutic indices are not exceeded to avoid endangering the patient.

DDIs can be caused by the inhibition or induction of enzyme(s) or transporter(s). Much is understood around DDI associated with the Cytochrome P450 enzymes, i.e CYP3A4 and CYP2D6 [54], but the knowledge and appreciation of DDIs with respect to drug transporters is less well known but growing [55].

Statins are widely prescribed drugs and since the treatment is life-long, many patients benefiting from statins are likely to be prescribed other medications, thus raising the potential for DDIs. For example, co-medication of statins with drugs used to treat infections such as itraconazole, ketoconazole, clarithromycin which are known to inhibit CYP3A4, can significantly increase (up to 20-fold) the circulating concentrations of atorvastatin, lovastatin and simvastatin [31]. Such elevated exposure to statins could potentially lead to muscle toxicity. Conversely, drugs that are inducers of CYP3A4 (e.g. the anti-seizure carbamazepine) will decrease the exposure and efficacy of statins undergoing CYP3A4 mediated metabolism (Kryland 2000).

Interactions with drug transporters have potential ramifications because of their important roles in the disposition of statins, especially for those with limited or no CYP-mediated metabolism e.g pravastatin. Gemfibrozil, another lipid lowering drug, can inhibit both OATP1B1 and OATP1B3, which led to the withdrawal of cerivastatin, due increased risk of rhabdomyolysis, when co-administered with gemfibrozil [56]. The DDIs between statins and the immunosuppressant agent cyclosporine are well documented, with circulating concentrations of statins increasing from 2- to 20-fold. Cyclosporine has been found to be an inhibitor of multiple transporters involved in statin disposition i.e. NTCP, OATP1B1, OATP1B3, OATP2B1, MRP2 but also inhibits CYP3A [32].

1.6 Utilisation of Membrane Vesicles to Investigate Drug Transport and Inhibitory Effects on Efflux Transporter

In vitro assays for studying the transport and inhibitory effects of a drug on transporters range from sandwich-cultured hepatocytes (SCH) to isolated plasma membrane vesicles. Sandwich-cultured hepatocytes are an *in vitro* tool for investigating the interplay of uptake and efflux of a drug and/or assessment of biliary clearance because they contain the characteristics of hepatocytes, including the canaliculi [57]. However, being a complex system, the ability to assess one substrate against a single transporter is challenging. In addition, these cells are not a viable method for standalone measurements of drug efflux because the drug must be taken into the cell by first intent.

Preparations of membrane vesicles over-expressing a single transporter are excellent systems for understanding either uptake or efflux transporter-drug interactions. During preparation there is a natural abundance of membranes that are formed inside-out (5-10%) [58]. Centrifugation of the membrane preparations separates out right-side out vesicles from inside-out vesicles [59]. For inside-out membranes expressing ABC transporters, the binding sites for ATP and substrate are now on the outside, consequently substrate transport occurs from the outside inwards. This *in vitro* model is therefore configured to transport drugs into the vesicular compartment for uptake and efflux transporters alike. There are two main expression lines used;

i. Spodoptera frugiperda (Sf9) insect-based membrane vesicles are produced by infecting the insect cells with baculoviruses carrying the gene expression for a transporter. The expression of transporter is high with very low levels of background expression of native transporters [60]. However, the level of cholesterol in the insect membranes is significantly lower than in mammalian membranes, which is known to regulate the

transporter activity [61]. Therefore, transport in these membranes maybe under-predictive compared to mammalian-based membranes.

ii. Mammalian membrane vesicles are generated from cell lines such as Chinese Hamster Ovary (CHO) or Human Embryonic Kidney 293T (HEK-293) which transiently over-express transporters. Although protein expression is lower than that derived from insect–based systems, mammalian membrane vesicles offer several advantages. The potentiating effect through the presence of cholesterol and its impact on substrate specificity generally results in greater signal-to-noise [62, 63]. In addition, proteins expressed in mammalian cells retain the full range of post-translation modifications (PTM), such as extensive N- and O-linked glycosylation. It is known that these PTMS can affect the functional expression of transporters which in turn will influence parameters such as Km and Vmax [64, 65].

These membrane preparations have been used to study transport in several assay formats. Two of the most applicable are the vesicular transport and ATPase assays.

1.6.1 Vesicular Transport Assay (Direct)

Following incubation with the transfected inside-out vesicle membranes, ATP dependent uptake of substrates will be captured into the vesicles (Figure 1.4). The vesicles are then separated from the incubation solution by rapid-filtration, with the vesicles remaining on the filter. This assay lends itself to the most quantitative techniques. If the substrate is radiolabelled or fluorescently tagged, then it can be measured directly from the filter plate. For unlabelled analytes quantification by methods such as LC-MS/MS can be performed following elution of the trapped analyte from the filter plate with a suitable solvent [66].

The vesicular transport assay has the advantage of enabling direct measurement of drug transport and affords itself well to determining kinetic parameters. However, if the substrate

has high-passive permeability then back diffusion (e.g. out of the vesicle) may lead to variability or false negatives.

Figure 1.4. Schematic of vesicular transport. X denotes transporter substrate passing through membrane-bound transporter (blue tubes) into vesicle (green circle), utilising ATP conversion into ADP as energy source. The extent of transport is determined by measuring the intra-vesicular concentration.

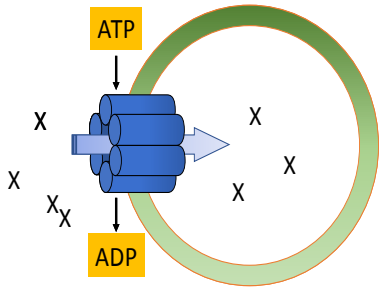

Inhibitory effects can also be evaluated by the vesicular transport assay format by measuring the uptake of a known control substrate in the presence of a potential inhibitor. Any inhibition will result in a decrease in the measurement of a probe substrate within the vesicle. To allow an unbiased parameter estimation regardless of the transporter mechanism (competitive vs non-competitive), the probe substrate concentration used needs to be significantly lower (5 to 10-fold) than its Km for the transporter of interest.

Probe substrates for these assays are often radiolabelled or fluorescently tagged to simplify quantification; this is because the inhibitor itself is not measured directly, rather it is the effect of the inhibitor on the probe substrate transport that is measured. Another disadvantage of this system is batch-to-batch variability, which can lead to differences in transporter expression, although cryopreservation has allowed for larger batches to be stored with minimal loss of activity [67].

1.6.2 ATPase Assay (Indirect)

The transport of compounds by ABC transporters is ATP-dependent requiring the hydrolysis of ATP to ADP *via* loss of a phosphate group (P_i). The rate at which the hydrolysis occurs is modulated in the presence of compounds that interact with the transporter [68]. A

colorimetric assay can be used determine the rate of P_i formation as an indirect measurement of the uptake of compound [69].

Figure 1.5. Schematic of ATPase assay. X denotes transporter substrate passing through membrane-bound transporter (blue tubes) into vesicle (green circle), utilising ATP conversion into ADP as energy source. The extent of transport is determined by measuring the phosphate (Pi) concentration.

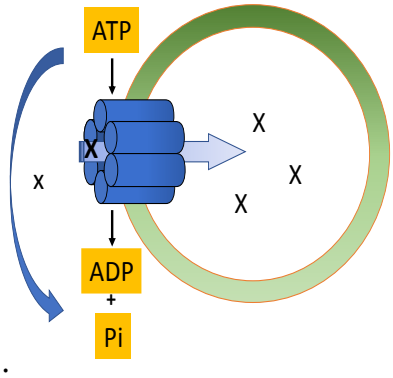

As with the vesicular assay, the transporter must be accessible to the incubation buffer, however, there is no requirement for a vesicular compartment since ATP activity is measured on the outside. Subsequently, the membrane permeability of a compound is not important for this assay format.

The obvious disadvantage of this assay is that transport activity is measured indirectly, and false positives can also occur when compounds stimulate ATPase but are not transported.

1.7 Kinetic Parameters Describing Drug Transport

The Michaelis-Menten model (Equation 1.1) was developed to describe enzyme kinetics, but the concept can also be relevant to transport processes (for modeling kinetic parameters). The formation of a substrate-transporter complex is similar to the enzyme-substrate complex, where by way of analogy, the transport velocity (cf reaction velocity) reaches a plateau (Vmax) after following a log type curve (Figure 1.7). Similarly, the affinity constant between transport protein and substrate (Km) would be equal to the concentration of the substrate when the transport velocity is half its maximum value.

Figure 1.6. Graph to show relationship between Km, Vmax and passive diffusion

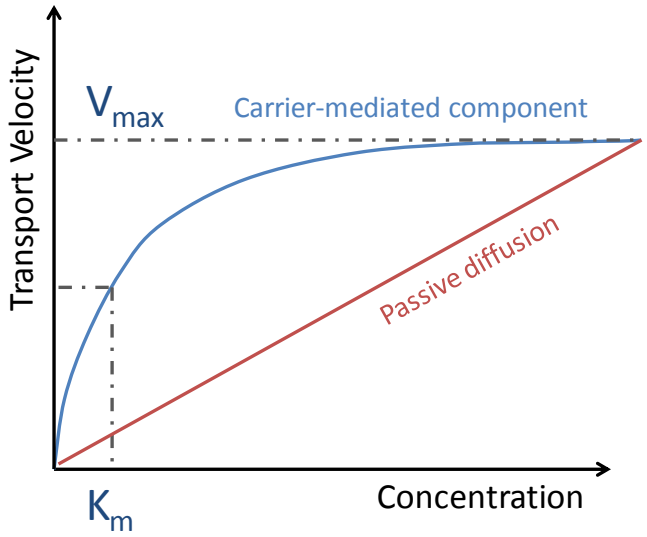

Equation 1.1. Michaelis-Menton

$$v = \frac{V_{max}[S]}{(K_m) + [S]} + P_{diff}[S]$$

When inhibition of the transporter occurs through the presence of a drug substrate, conducting a series of uptake and inhibition studies (varying the concentrations of inhibitor and substrate) allows the determination of the inhibitory constant Ki

Equation 1.2. Determination of Ki

$$K_i = \frac{IC_{50}}{1 + \frac{[S]}{K_m}}$$

1.8 Quantitative Techniques

1.8.1 Fluorescence

Fluorescent emission can be viewed as a form of luminescence. The fluorescent molecule absorbs a photon from light, which then induces an excited electronic state. As the molecule returns back to the lower energy ground state, heat is released along with emission of a

photon of lower energy (and therefore of longer wavelength). This process can be exploited to detect molecules with suitable fluorescent properties, examples being positive or negative controls in *in vitro* experiments.

A limited number of molecules are natively fluorescent (versus UV absorbance), which enables signal detection to be characterised by low background and high selectivity. In general, conjugation (e.g. *via* double bonds) improves fluorescence intensity, however, the synthesis of suitable molecules must take account of the excitation and emission wavelengths not interfering with one another. Conversely, the limited number of structural moieties able to yield a fluorescent response limits its applicability much more than techniques such as mass spectrometry [70].

1.8.2 Radiolabelled Detection

This form of detection relies on the inherent instability of certain isotopic forms of atomic nuclei, such as carbon-14. This instability arises from an imbalance in the ratio of protons to neutrons in the atomic nucleus that ultimately leads to emission of both particles and energy from the nucleus. Although present in trace amounts in nature, carbon-14 can be made in concentrated form as a by-product of nuclear reactors, forming barium carbonate that can then be converted to carbon dioxide and used as a precursor in synthetic chemistry to boost the ^{14}C content in more complex organic molecules. Isotopes do not differ in chemical properties relative to stable isotope versions of the same element (the number of protons determines the number of electrons, which in turn determines the chemical characteristics).

The nuclear decay of a radiolabelled compound can be detected by processes able to absorb the emission and then convert this to a measurable signal, e.g. scintillation. Radiolabelled compounds can be hazardous to handle and/or synthesise and hence the amount of radioactivity (specific activity) needs to be balanced carefully against the ability to observe a

detectable signal over background levels. The storage, tracking and disposal of radioactive compounds is also tightly controlled by national regulations making their use more cumbersome than other 'cold' approaches [71].

1.8.3 Mass Spectrometry

Detection and quantification by mass spectrometry (MS) has become an important part of modern bioanalysis. MS systems are often 'hyphenated' with techniques such as high-performance liquid chromatography (HPLC) that allows the separation of analytes of interest from complex sample preparations followed by selective and sensitive MS detection.

Figure 1.6 shows the setup of HPLC and MS (specifically tandem MS or MS/MS) used in this thesis to quantify statins and positive control substrates. High specificity for detection of the analyte is gained through a series of steps, each adding a different element of selectivity (Figure 1.6).

a. Chromatographic separation of the analyte is based on its competing physicochemical interactions with the stationary phase and mobile phase. Like many organic small molecules used as drugs, statins are sufficiently lipophilic to be separated using reversed phase HPLC C18 analytical column.
b. Following ionisation of the species present in the HPLC eluent, the analyte of interest is selectively transmitted through to the next MS region while other components are discarded. Electromagnetic fields are applied to manipulate the ionic species whose trajectories through the MS are determined by their mass-to-charge (m/z) ratios. Essentially this first step of MS selection is a molecular weight filter. The most common ionisation process coupled to HPLC is electrospray, which is relatively 'soft' and tends to protonate or deprotonate analytes without imparting enough internal

energy to induce fragmentation. In the case of statins, the acidic nature of the chemical template favours the deprotonated species $[M-H]^-$.

c. The isolated ionic species often referred to as the precursor (or parent) ion is then subjected to an excitation process in order to induce the formation of product (or fragment) ions. A highly abundant product ion is then selectively transmitted through to the detector (based on its m/z ratio) while other components are discarded. Essentially this step is a structural filter. Excitation is caused by accelerating the mass selected analyte ion into a cloud of chemically inert gas (e.g. nitrogen or argon). Each low energy collision between analyte and gas causes a small amount of the analyte's kinetic energy to be converted into vibrational energy. This slowly 'heats' the ion to a point where bonds can cleave leading to structurally informative fragments.

d. In the final detection step, the product ion is accelerated into an electron multiplier inducing an electric current that can then be captured by the MS data system. The electric current produced is proportional to the number of ions hitting the detector, which allows the technique to be quantitative. However, the ionisation and fragmentation processes are chemical in nature and vary from molecule to molecule. Therefore, chemical reference standards are needed to construct a calibration curve for each specific analyte.

e. Based on this process, only analytes with the appropriate HPLC retention time, precursor m/z ratio and product m/z ratio will be integrated and quantified.

Figure 1.6: Schematic of the analysis by HPLC-MS/MS. Sample is injected onto a chromatographic column where separation of analytes occurs due to their different physicochemical properties. Following elution from the column into the mass spectrometer, heated desolvation of the liquid and ionisation of small droplets results in the formation of charged gaseous species. The charged parent mass of interest is then selected in the first quadrupole (Q1). This ion is then passed into the collision cell (Q2) where it is bombarded with high energy inert collision gas ($N_{2)}$ and fragmented. Theses ions are passed into the third quadrupole (Q3) where the most dominant fragment ion is selected as the product ion.

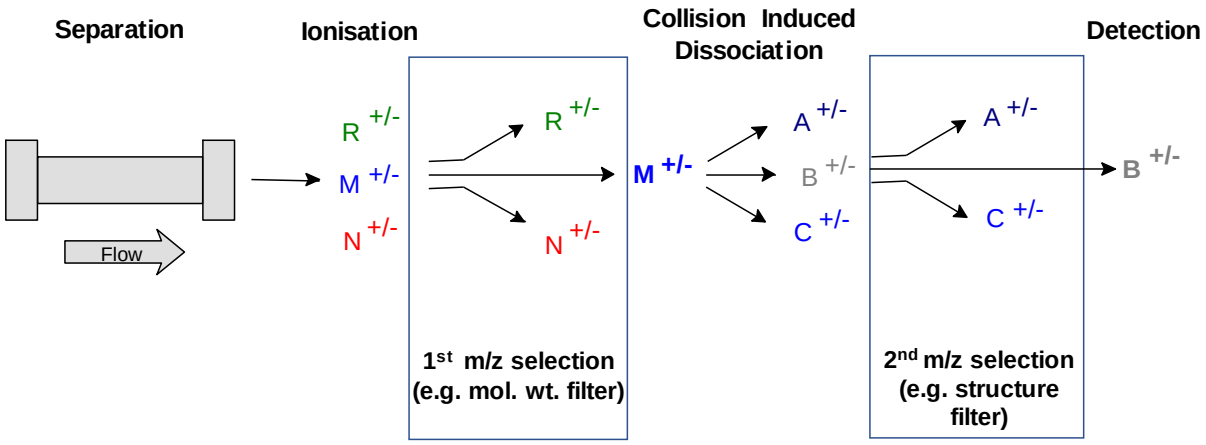

1.9 Experimental Aims

Statins have become a common medication, therefore understanding the disposition and potential DDIs between statins and other prescribed medication /drug candidates is of clinical importance. The aim of this work was to determine whether statins are substrates and/or potential inhibitors of MRP2, MRP3 and MRP4, utilising membrane vesicles containing the transporter under scrutiny. This work examined seven commercially available and commonly prescribed statins, namely atorvastatin, fluvastatin, lovastatin rosuvastatin, simvastatin, pitavastatin, pravastatin and cerivastatin (which is discontinued due to fatal DDIs). The following experiments were conducted:

- **Aim 1**: Implementation of suitable probe substrates to enable analysis by LC-MS/MS
- **Aim 2**: Pilot assessments to determine which statins are substrates against MRP2, MRP3 and MRP4
- **Aim 3**. Validation of analytical methods for statins determined to be substrates in support of kinetic analysis.
- **Aim 4**: Kinetic studies for statins determined to be substrates (Km/Vmax).
- **Aim 5**: Evaluation of statins as inhibitors of MRP2, MRP3 or MRP4

Experimental

1.10 Material and Methods

1.10.1 Chemicals

Atorvastatin acid, fluvastatin acid, cerivastatin acid, pravastatin acid, ATP (adenosine triphosphate disodium salt), AMP (adenosine monophosphate disodium salt, Tris-Base (Tris[hydroxymethyl]aminomethane, magnesium chloride, sodium chloride, sucrose, bovine serum albumin, dehydroepiandrosterone sulphate (DHEAS), estradiol-17-β-D-glucuronide ($E_2$17βg) and MK-571 were purchased from Sigma-Aldrich (Gillingham, UK). Lovastatin acid, pitavastatin, and simvastatin acid were purchased from Cambridge Bioscience, (Cambridge, UK) and rosuvastatin was obtained from Sequoia Research products (Berkshire, UK).

PREDIVEZ™ transporter kits (SOLVO Biotechnology Szeged, Hungary) were used for investigation of transport with MRP2 and MRP3 alongside associated protocols. Kits contain membrane vesicles prepared from recombinant baculovirus infected Sf9 insect cells expressing the human MRP2 or MRP3 transporter, utilising 5(6)-Carboxy-2',7'-dichlorofluorescein (CDCF) and benzbromarone (BB) as control substrate and inhibitor, respectively. For the investigation of transport against MRP4, vesicle membranes (SOLVO Biotechnology Szeged, Hungary) prepared from recombinant baculovirus infected HEK293 cells expressing the human MRP4 were used alongside the supplied assay protocol [72]. Millipore multiscreen HTS 96 well filter plates (MSFBN6B10) were used for filtration.

1.10.2 General Protocol for the Uptake Experiments.

Initial stocks were prepared in DMSO for each statin (30 mM), MK-571 (30 mM), $E_2$17βg (10 mM) and DHEAS (5 mM). Assays were performed using membrane vesicles (50 μg) with assay reagents provided in kits for MRP2/ MRP3. Assay buffers were prepared for MRP4 as described in the protocol supplied by SOLVO Biotechnology [72]. Following pre-incubation of vesicles (10 to 15 min), reactions were initiated by the addition of either MgATP (10 mM) or MgAMP (10 mM) solutions. All analyses were performed with individual replicates of three unless otherwise stated. The SOLVO protocols used were modified to suit the laboratory instrumentation e.g. HPLC-MS/MS. There were no major deviations from the protocols supplied with the vendor's kit, except for using non-radio-labelled (cold) substrates.

Non-radio-labelled $E_2$17βg was used as a probe substrate for MRP2, MRP3 and MRP4. At the end of the incubation, ice cold washing buffer was added to terminate transport, supernatants were transferred to 96-well glass fiber filter plates, vacuum suction was then applied, and all wells washed with 5 cycles of washing buffer. The filter plates were dried at 37ºC (10 min), after which 100 μL of methanol was added to all wells and the plates were then incubated at room temperature for a further 10 min. The methanol was drawn into a 96-deep well protein Lowbind Eppendorf block *via* vacuum suction. The resulting lysate was evaporated to dryness under a stream of nitrogen gas (40ºC) followed by reconstitution in 100 μL 50/50 v/v acetonitrile/water containing an in-house generic internal standard (SB-243213). The amounts of statins and $E_2$17βg were determined by means of LC-MS/MS. A schematic of the methodology is shown in Appendix 1.

1.10.3 Optimisation of mass spectrometer (MS) parameters

Optimisation of the mass spectrometer parameters was performed by infusing solutions of each statin, DHEAS and $E_2$17βg at approximately 20 ng/mL in 5 mM ammonium bicarbonate/acetonitrile (1:1 v/v) at a flow rate of 0.8 mL/min. During infusion, m/z ratios of the parent $[M-H]^-$ ions were noted and subjected to collision-induced dissociation to determine the most abundant product ion. The key parameters, the ion-spray (IS) voltage, source temperature, delustering potential (DP) and collision energy (CE) were optimized for each analyte and used to generate the multiple reaction monitoring (Appendix 2).

1.10.4 Set up of Liquid Chromatography (LC)

Following the optimization of the MS, a variety of different mobile phases and elution gradients were assessed. This was to enable the analysis of all the statins, DHEAS and $E_2$17βg without comprising the response, chromatographic peak shape and retention for each. Final optimised chromatographic conditions are shown in Appendix 3.

1.10.5 Implementation of DHEAS and $E_2$17βg as Probe Substrates for analysis by LC-MS/MS.

Probe substrates are drugs or endogenous analytes that have known affinity for a transporter. They are used in vesicular-based assays to validate the system. Current methodologies for MRP2, MRP3 and MRP4 vesicular transport assays, mainly incorporate radio-labelled or fluorescence probe substrates, such as CDCF. Here non-radio-labelled $E_2$17βg and DHEAS were assessed as probe substrates employing LC-MS/MS as the detection method for quantification. $E_2$17βg and DHEAS were incubated in triplicate with both MgATP and MgAMP. Incubation concentrations and times were based on radio-labelled methodologies [73]. These methodologies are suitable to investigate both uptake and inhibitory effects of a substrate. $E_2$17βg was incubated at 50, 1 and 10 μM, with MRP2, MRP3 and MRP4, respectively. DHEAS was incubated with MRP4 at a concentration of 0.5 μM.

Following LC-MS/MS analysis, the data were inspected to assess whether this detection method was reliable e.g. by reviewing signal to noise of analyte response, variability of triplicates and fold differences in accumulation of the control substrates in incubations with ATP compared to AMP. Table 2.1 shows incubation conditions for $E_2$17βg and DHEAS and CDCF (previously determined by fluorescence).

Table 2.1 Km values for positive controls CDCF, $E_2$17βg and DHEAS against each transporter and incubation condition used for each experiment.

Transporter	Substrate	Km values of Substrates	Incubation conc.	Pre-incubation time	Incubation time
MRP2 (ABCC2)	$E_2$17βg	113-400 μM [74, 75]	50 μM	10 mins	10 mins
	CDCF	22 μM [76]	5 μM		30 mins
MRP3 (ABCC3)	$E_2$17βg	20-52 μM [75, 77]	1 μM	10 mins	20 mins
	CDCF	56 μM[76]	5 μM		10 mins
MRP4 (ABCC4)	$E_2$17βg	46-87 μM [41, 78]	10 μM	10 mins	10 mins
	DHEAS	2 μM [42]	0.5 μM	15 mins	5 mins

1.10.6 Method Development and Validation of Analysis by LC-MS/MS

For the pilot assessments of statins (2.1.8.1), only semi-quantitative data was required for analysis of the data where the LC/MS/MS responses of uptake from substrates incubated in the presence of ATP relative to AMP was required. For these experiments, the responses were confirmed to be within the linear range of the MS detector and the Internal Standard (I.S) signal was consistent throughout the analytical run.

For the determination of Vmax and Km (fluvastatin, pitavastatin, pravastatin, rosuvastatin and $E_2$17βg probe substrate), a series of additional experiments were performed to characterise the method (see below).

1.10.7 Assessment of Linearity and Sensitivity

With limited amounts of control vesicles, stock solutions (5mM in DMSO) were prepared for fluvastatin, pitavastatin, pravastatin, rosuvastatin and $E_2$17βg, then diluted further to give working solutions as detailed in Appendix 4. Calibration standards were then spiked over the concentration range of 0.1 to 1000 nM according to Appendix 4. 100 µL duplicate aliquots were placed in a low protein binding 96 deep well plate for analysis by LC-MS/MS. Following data processing of the chromatographic responses, the lower limit of quantification (LLQ) for each analyte was defined as the minimum concentration achieving a signal to noise ratio ≥ 5:1.

The final calibration ranges (see section 2.1.6.5) were selected to be linear from the assay LLQ to the upper limit of quantification (ULQ) applying a weighted 1/(x*x) linear regression.

1.10.7.1 The Effects of Matrix Components on LC-MS/MS Response

The LC-MS/MS response of an analyte can be affected by so-called 'matrix effects' whereby co-eluting endogenous components compete for charge during the ionisation process. The presence of matrix effects was assessed by comparing the responses of post-extracted samples (n= 6 replicates) of SB-HEK293-Mock-CTRL vesicles spiked with each of the statins at either 0.5 or 200 nM, against equivalent samples prepared with assay buffer only. Figure 2.1 shows a scheme for the sample preparation.

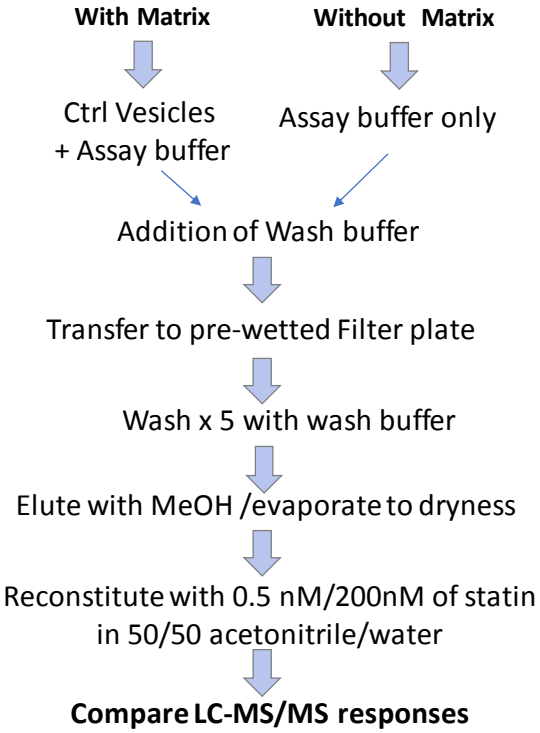

Figure 2.1. Schematic of sample preparation for assessments of Matrix effects.

The effect of matrix on the LC-MS/MS was then calculated using the following equation:

$$\text{Matrix Effect (ME)} = \frac{A-B}{A} X\ 100$$

Where A = Mean response of analyte without matrix

B = Mean response of analyte with matrix

In addition, the precision of the samples containing matrix were assessed to ensure they were ≤ 15% at all concentrations.

1.10.7.2 Non-Specific Binding to Filter Plates and Vesicles

Non-specific binding (NSB) is the unwanted adsorption/binding of an analyte to experimental material or equipment that can result in an underestimation of results. To assess the impact of NSB of the statins and evaluate the implementation of a possible anti-adsorption agent (0.1% bovine serum albumin (BSA) or 100 µM atorvastatin), samples were prepared according to Figure 2.2. Experiments employed SB-HEK293-Mock-CTRL vesicles with n=4 replicates for each statin per pre-wet condition

Figure 2.2. Schematic of sample preparation for assessment of NSB

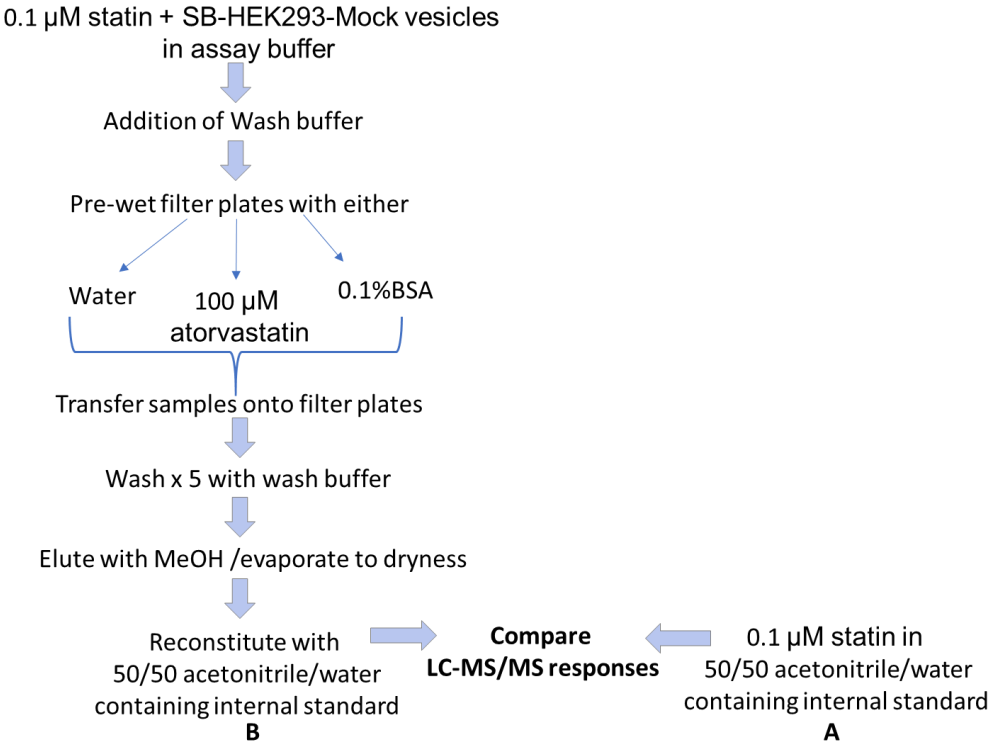

The % of NSB for each pre-wetting filter conditions was calculated using the following equation:

$$\% \text{ NSB} = \frac{B}{A} X\ 100$$

A = Mean response of 0.1 µM statin in 50/50 acetonitrile/water

B = Mean response of 0.1 µM statin following extraction

1.10.7.3 Preparation of Control Matrix

To a scaled-up volume of HEK293-Mock-CTRL membrane vesicles in assay buffer, Mg-AMP and wash buffer were added proportionally (1:0.5:4) to that of a single individual incubate. Approximately 300 µL aliquots were transferred onto pre-wetted filter plates which were washed, eluted with methanol and evaporated to dryness. The dried down residual lysate was subsequently used for the preparation of the validation run(s) and the preparation of calibration standard for the analysis of statin kinetic parameters Vmax/Km.

1.10.7.4 Linearity, Precision and Bias (P&A) of Assay (With Matrix)

5 mM stock solutions (A and B) of fluvastatin, pitavastatin, pravastatin in DMSO were prepared. These stocks were diluted together with DMSO to give a 1mM stock consisting of all four statins (Table 2.2). For $E_2$17βg 1 mM A and B stocks were separately prepared in DMSO

Table 2.2 Preparation of 1mM combined statins working solutions

Working Solutions	Statin	Dilution factor	Volume of 5 mM Stock (µL)	Make up Volume of DMSO (µL)	Final Concentration (mM)
A1/B1	Rosuvastatin	X 5	50 µL of each	50	1mM
	Pitavastatin				
	Pravastatin				
	Fluvastatin				

To confirm the linearity of the methods calibration standards were prepared in duplicate from the 1mM A stocks, covering the concentration ranges of 0.25 to 250 nM and 1 to 1000 nM for statins and $E_2$17βg, respectively. To assess precision and accuracy 5 levels of validation samples were prepared from the 1mM B stocks at the following nominal concentrations;

i. At the LLQ
ii. 3 x the LLQ
iii. Midpoint of Calibration Range
iv. 75% to 80% of the HLQ
v. At 100% of the calibration range

n= 6 replicates were analysed per validation level against calibration lines

Calibration standards and validation samples were both prepared utilising the D300e (TECAN, Switzerland)). This automated system was used to dispense volumes ranging from 0.025nL to 100 nL from the 1mM solutions directly into 96 deep well Eppendorf plates

containing control matrix (see section 2.3.2.4). To control blank matrix" Total Blanks" 100 µL of 1:1 (v/v) acetonitrile: water was added and to all other samples 100 µL of 1:1(v/v) acetonitrile: water containing internal standard. Samples were analysed by means of LC-MS/MS.

1.10.7.5 Stability of $E_2$17βg

$E_2$17βg was spiked at 1 and 50 µM into assay buffer, n=6 replicates (50 µL) from each concentration were taken as T= 0 samples. Following incubation at 37°C for 30 mins, an additional n = 6 replicates (50 µL) were taken from each concentration. To the samples 200 µL of 1:1 (v/v) acetonitrile: water containing internal standard was added and samples analysed by LC-MS/MS.

1.10.8 Uptake of Statins in vesicles expressing MRP2, MRP3 or MRP4

1.10.8.1 Pilot Experiments

Pilot assessments were conducted to determine if ATP-dependent uptake of atorvastatin acid, cerivastatin acid, fluvastatin acid, lovastatin acid, pitavastatin acid, pravastatin acid, rosuvastatin acid and simvastatin acid in MRP2, MRP3 and MRP4 could be detected in vesicles over-expressing MRP2, MRP3 or MRP4 [66]. Experiments were performed at two statin concentrations (low and high): 1 and 10 µM; and at two incubation times (short and long): 2 and 10 min for MRP2, 5 and 10 min for MRP3 and 5 and 10 min for incubations with MRP4 using the SOLVO methods.

Statins were considered to be a substrate if they elicited ≥2-fold difference in accumulation in incubations with ATP compared to those with AMP or if this difference was deemed to be statistically significant when applying a Students *t*-test ($P<0.05$). For statins identified as substrates, kinetic parameters were then investigated.

1.10.8.2 Time Dependent Experiments-Determination of Vmax

Time-dependent experiments (combinations shown below table 2.3) were carried out to determine the linear phase of transport. Statins were incubated at low concentration (1 μM) with incubation times of 1, 2.5, 5, 10, 15, 20 and 30 min. Each time point was measured in triplicate.

Table 2.3 Combinations of statin vs transporter time-dependent experiments conducted

Transporter	Statin (1 μM)
MRP2	Rosuvastatin
MRP3	Pravastatin Rosuvastatin
MRP4	Fluvastatin Pitavastatin Rosuvastatin

1.10.8.3 Determination of Km

Pravastatin was preincubated for 10 mins at 0.14, 0.41, 1.22, 3.67, 11, 33 and 100 μM then incubated for 5 mins following addition of either MgATP or MgAMP. Kinetic constants (Km) were determined for pravastatin within the concentration range of 0.14 μM to 100 μM of statin at an incubation time determined from the linear phase of the time-dependent experiments. All incubations were performed in triplicate and analyzed against calibration standards prepared over the ranges of 0.25 to 250 nM.

1.10.9 Inhibitory effects of Statins on MRP2, MRP3 and MRP4 mediated Transport of Probe Substrates

Quadruplicate incubations of all the statins were prepared at 0, 4.7, 9.4, 18.8, 35.7, 75, 150 and 300 μM (utilizing the D300e) with the probe substrate CDCF (5 μM) for MRP2 and MRP3 and $E_2$17βg (10 μM) for MRP4. Benzbromarone (BB) and MK571 were also incubated alongside as positive control inhibitors for MRP2/ MRP3 and MRP4, respectively.

Table 2.4 details the conditions for each probe substrate against the appropriate transporter and the associated probe inhibitor.

For the measurement of passive transport, additional quadruplicate incubations were conducted for probe substrates; CDCF (5 μM) or $E_2$17βg (10 μM) in the presence of MgAMP (4 mM). Following incubation at 30, 10 and 20 minutes for MRP2, MRP3 and MRP4, respectively, reactions were terminated, and filtration conducted as per protocols. After final washing, the filter plates were dried at 37ºC (10 min), 100 μL of 0.1N NaOH was then added to MRP2 and MRP3 plates and 100 μL of methanol to MRP4 plates. Plates were further incubated at room temperature (10 min) and the lysates for MRP2 and MRP3 then eluted into black 96-well clear bottom plates for fluorescence quantification (excitation 485nm, emission:538 nm, Victor2 Fluorometer, PerkinElmer life Analytical sciences). Lysates for MRP4 were evaporated to dryness then reconstituted in 100 μL of acetonitrile: water (1:1 v/v) containing internal standard (I.S) (SB243213) for analysis by LC-MS/MS.

Table 2.4 Conditions for each probe substrate against the appropriate transporter and the associated control inhibitor

Transporter	Probe Substrate	Probe Inhibitor	Pre-incubation time	Incubation time	Detection
MRP2/MRP3	CDCF (5μM)	BB	10 mins	30/10 mins	Fluorescence
MRP4	$E_2$17βg (10 μM)	MK571	10 mins	20 mins	LC/MS/MS

1.10.10 Analysis of Substrates by HPLC-MS/MS

Sample aliquots for each statin (5uL) were injected onto a Acquity™ BEH C18 column (50 x 2.1 mm, (Waters, Elstree, UK) and eluted under reversed phase LC conditions; mobile phase A consisted of ammonium bicarbonate (5 mM), mobile phase B was acetonitrile. Initial gradient conditions of 5% B were held for 0.2 min, ramped to 70% B (0.2 min to 1.2 min), ramped again to 95% B (1.2 to 1.6 min) then re-equilibrated to 5% B (1.6 to 2.0 min). Liquid eluent was directed to a Sciex API5000 tandem quadrupole mass spectrometer (Applied

Biosystems, Warrington UK) coupled to a TurboIonspray™ interface. Statins and the I.S were detected in negative polarity *via* multiple reaction monitoring (MRM) mode. (Appendices 2 and 3).

1.11 Utilisation of D300e Digital Dispenser

The D300e was programmed with the following top stocks prepared in DMSO to dispense directly from;

- 1mM for statin and $E_2$17βg validation and standard line preparations.
- 300 mM for inhibitory effects of statins, BB and MK571.

The D300e was programmed within minutes using a simple "Excel" based 96-well plate layout with the analyte and concentrations required. The D300e automatically determined the volume of the stock required for each well then when requested prepared the plates as required (30 secs/per 96 well plate).

1.12 Data Analysis

For the initial pilot experiments, relative quantification was performed using chromatographic peak area ratios (analyte-to-I.S.), arithmetic means and standard deviations were derived. For kinetic analysis, absolute quantification was performed against standard curves (nM).

ATP-dependent uptake was calculated by subtracting the statin concentration in the presence of AMP from statin concentration in the presence of ATP and converting these results to pmoL/mg/min. Kinetic parameters (Km and Vmax) were then determined with non-linear regression-fitting of ATP dependent transport to the Michaelis-Menten equation from three independent experiments (Graphpad Prism v7.04).

IC_{50} values for the inhibition of CDCF and $E_2$17βg by statins were calculated by subtracting the level of transport determined from ATP incubations from the basal level of control

substrate with AMP and using the Hill equation (variable slope using Graphpad Prism® v7.04) to obtain best-fit parameters.

1.12.1 Calculations and Statistical Analysis

The following calculations were used throughout the experimental analysis.

1. Mean measured concentrations ($\bar{x}$) and standard deviaiton (SD) for each set of replicates
2. Bias

$$\left(\frac{\bar{X}}{actual\ concentration} \times 100\right) - 100$$

3. % Accuracy

$$\left(\frac{acutal\ concentration}{mean\ concentration}\right) \times 100$$

% accuracy at all concentrations should be within ≤15% (≤20% at the LLQ).

4. Coefficient of variation (CV) for a set of replicate samples at a known concentration.

$$\left(\frac{SD}{\bar{X}}\right) \times 100 = \%\ \text{CV}$$

% CV at all concentrations should be ≤15% (≤20% at the LLQ).

5. Inhibitory effects were calculated of % transport of positive control

$$\left(\frac{ATP\ dependent\ transport\ in\ the\ presence\ of\ test}{ATP\ dependent\ transport\ in\ drug\ free\ control}\right) \times 100$$

6. Students *t*-test

   Determinations of statistically significant difference between uptake for incubations with ATP vs AMP were derived using a Students *t*-test (unpaired) with a 95% confidence (GraphPad Prism 7.04).

   A statistical difference was considered at a calculated P value <0.05.

2 Results

2.1 Optimisation of LC-MS/MS Conditions

Details of the LC-MS/MS methods developed for the analysis of $E_2$17βg and DHEAS are shown in Appendix 3.

2.2 Evaluation of DHEAS and $E_2$17βg as probe substrates for analysis by LC-MS/MS

Uptake of $E_2$17βg was observed against all three transporters with 10.7-, 13- and 5.8-fold differences between incubations with ATP vs AMP for MRP2, MRP3 and MRP4, respectively (Figure 3.1). Similarly, following incubation with MRP4, a 5.2-fold difference in uptake of DHEAS was measured between ATP incubation vs AMP.

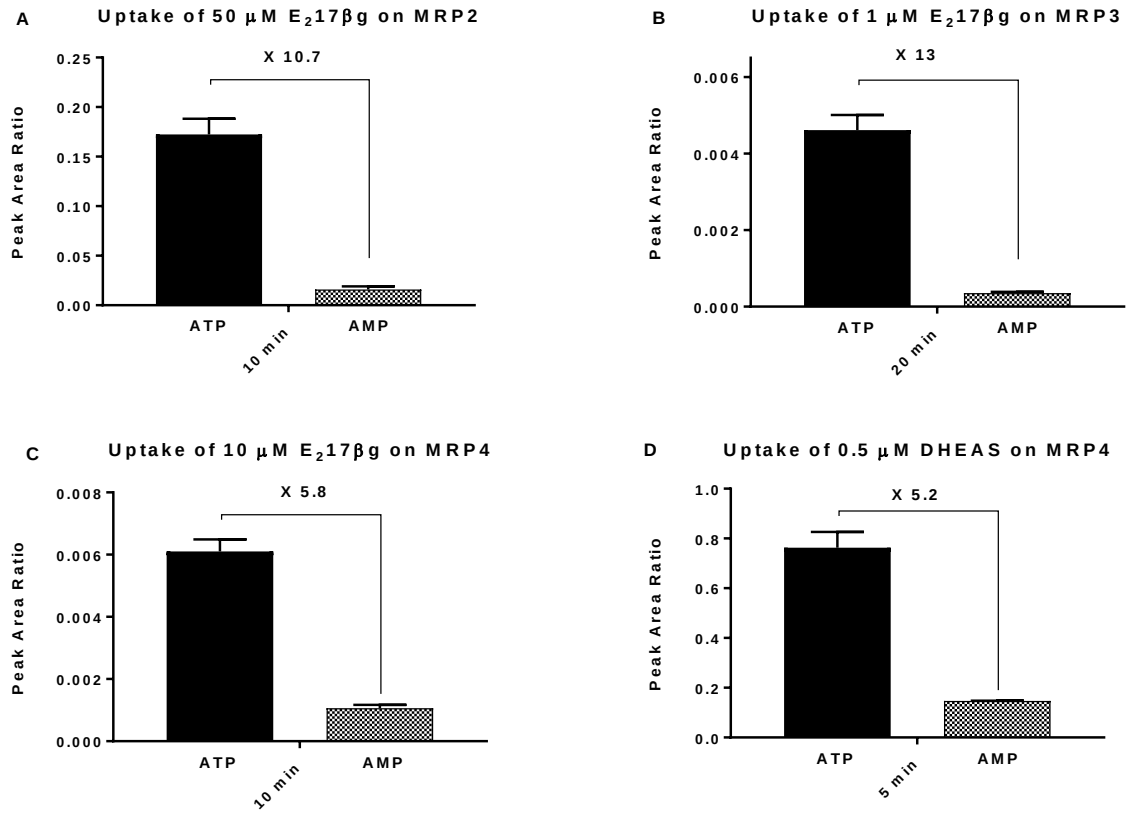

Figure 3.1. Uptake of $E_2$17βg following incubation with A) MRP2 at 50 µM for 10 min B) MRP3 at 1 µM for 20 min C) MRP4 at 10 µM for 10 min and the uptake of DHEAS following incubation with D) MRP4 at 0.5 µM for 5 min

The standard deviations from the triplicate analysis were low (≤20% of the-mean value) (see Table 3.1) and following review of the LC-MS/MS chromatograms, the smallest signal-to-noise ratio detected was 5:1 for uptake of $E_2$17βg on MRP3 incubated with AMP.

Table 3:1. Summary of results for the assessment of $E_2$17β and DHEAS as probe substrates for either MRP2, MRP3 and MRP4.

Transporter	**Positive Control**	**ATP Mean Ratio ±SD**	**AMP Mean Ratio ± SD**	**Fold Difference (ATP/AMP)**
MRP2	$E_2$17βg	0.172 ± 0.0158	0.0160 ± 0.00302	10.7
MRP3	$E_2$17βg	0.00461 ± 0.00040	0.00036 ± 3.34E-05	13
MRP4	$E_2$17βg	0.006103 ± 0.00039	0.00106 ± 0.000113	5.8
	DHEAS	0.763 ± 0.0633	0.147 ± 0.00577	5.2

Mean and SD quoted from n=3 replicates.

These results demonstrate that LC-MS/MS can be successfully applied for the analysis of $E_2$17βg and DHEAS, and that both these substrates are suitable probe for the relevant transporters. As $E_2$17βg was applicable to all three MRP transporters and it elicited a similar fold uptake as DHEAS for MRP4, it was deemed appropriate to solely use $E_2$17βg as the probe substrate for all. Additional experiments were performed to further characterise the method and reliability for $E_2$17βg, such as linearity, precision and accuracy and stability under experimental condition's (see sections 3.2.4 and 3.2.5).

2.3 Method Development and Validation of Analysis by LC-MS/MS

Pilots were used as a screening process to identify potential substrates. For these assessments, a low and high concentration of substrate was triturated against two-time points, comparing incubations with and without ATP. As these experiments were purely for ranking purposes prior to semi-quantification analysis, where peak: area ratios (PAR) of stain vs constant amount of internal standard area was considered sufficient for analysis. The greater the difference between PAR of ATP vs AMP incubation was relative to the greater fold indifference in transport between passive (AMP) and active transport (ATP).

2.3.1 Assessment of Linearity and Sensitivity

Initial assessment of the potential assay linearity and sensitivity for fluvastatin, pitavastatin, pravastatin rosuvastatin and $E_2$17βg were investigated. Calibrations of each analyte prepared in internal standard solution without matrix data demonstrated that 0.25 to 250 nM was an appropriate assay range for fluvastatin, pitavastatin, pravastatin and rosuvastatin. Over this range, the calibration lines were all linear with R^2 values of ≥0.9975 using a weighting of ($1/X^2$) and signal-to-noise values ≥ 10:1 for all analyte LLQs.

Similarly, for $E_2$17βg the assay range 1 to 1000 nM was observed to be suitable, with an R^2 value of 0.9986 using a weighting of ($1/X^2$) linear regression and a signal to noise of the LLQ (1 ng/mL standard) of approximately 7:1. The establishment of the appropriate quantifiable ranges directed the design of all other method validation experiments.

2.3.2 The Effects of Matrix Components on LC-MS/MS Response

The matrix effects (%) of co-eluting matrix components and the associated precisions (%CV) are summarised in Table 3.2. Individual replicate responses are detailed in Appendix 5. Matrix effects were observed for all statins at both 0.5 and 200 nM.

The % changes demonstrated an enhancement on the LC-MS/MS response (matrix present versus no matrix) which varied from -3.6% to 45.6% increasing from pravastatin → rosuvastatin → pitavastatin → fluvastatin. Interestingly, this increase was observed with an increase in lipophilicity of the statins. One way to circumvent the matrix effect would be to use a stable isotopically labelled (SIL) version of each of the statins and reassess peak area ratios. As there was no SIL available, in this instance, the %CV response samples containing matrix was ≤ 15% for all statins, demonstrating that although there was an effect on the signal it was variation was low. To overcome the matrix effect, calibration standards for sample analysis were prepared in control matrix.

Table 3:2. Summary of results for the assessment of matrix effects

Statin	**% Matrix Effect**		**%CV of Matrix**	
	0.5 nM	**200 nM**	**0.5 nM**	**200 nM**
Fluvastatin	45.6	32.2	8.9	9.8
Pitavastatin	26.9	22.8	11.8	10.8
Pravastatin	15.5	13.2	8.5	11.1
Rosuvastatin	-3.6	2.85	4.0	3.5

2.3.3 Non-Specific Binding (NSB) to Filter plates and Vesicles

The % of non-specific binding observed for the each of the statins versus pre-wetting conditions are summarised in Table 3.3. The % NSB observed was small (<2%) but evident for all statins ranging from 0.2 to 1.7%, increasing in the order pravastatin →rosuvastatin → pitavastatin →fluvastatin. The pre-wetting of the filters with 100 μM atorvastatin or 1% BSA versus water did not appear to have any impact on the degree of % NSB, presumably because of the low overall binding observed.

T**able 3:3**. % of Total Non-Specific Binding of Statins to Filter plates and Vesicles

Pre-wetting of Filter Plates	**% of NSB of 0.1 µM Statin**			
	Fluvastatin	**Pitavastatin**	**Pravastatin**	**Rosuvastatin**
100 µM atorvastatin	1.46	1.20	0.150	0.199
0.1% BSA	1.73	1.42	0.290	0.147
Water	1.11	0.783	0.311	0.174

2.3.4 Sensitivity and Linearity (with Matrix)

Linear responses in the analyte/internal standard peak area ratios were observed for fluvastatin, pitavastatin, pravastatin and rosuvastatin over the range 0.25 to 250 nM and for $E_2$17βg over the range 1 to 1000 nM. The calibration data presented in Appendix 6 show that the correlation coefficients obtained using linear-weighted ($1/X^2$) regression were ≥ 0.9924 for all analytes. Chromatograms of the LLQ for each analyte were assessed and the signal-to-noise ratios were deemed to be acceptable for all at ≥ 6:1. Representative calibration plots and chromatograms of the LLQs are shown in Appendices 7 to 11.

2.3.5 Precision and Accuracy of Assay

Concentrations of fluvastatin, pitavastatin, pravastatin, rosuvastatin and $E_2$17βg were determined from each of their respective calibration lines. For each validation level per analyte, the mean, standard deviation, % precision (%CV) and % accuracy was calculated. For all validation sample concentrations, the % precision values ranged from 5.62 to 17.7 %. The highest % precision of 17.7% was observed for pravastatin at the LLQ. At all validation sample concentrations, the % accuracies were within ±15% of nominal values. These data are within the defined acceptance criteria and confirm suitability of the methods for quantification of fluvastatin, pitavastatin, pravastatin and rosuvastatin (0.25 to 250 nM) and $E_2$17βg (1 to 1000 nM). Appendix 12 summarises the validation data for each analyte.

2.3.6 Stability of $E_2$17βg

$E_2$17βg is a conjugated glucuronide metabolite of estradiol which may have the potential to revert back to estradiol under certain conditions. The stability of $E_2$17βg was therefore assessed in assay buffer at 1 and 50 µM by comparing the mean concentrations from T=0 against the mean concentrations after 30 mins (T=30 mins) of incubation at 37°C. The % bias was less than 15% for both concentrations and time points, and the % difference between T=0 and T=30 samples were less than ± 3%. Results are shown in Appendix 13 and confirm the stability of $E_2$17βg under the experimental conditions employed.

2.4 Statins as Substrates for human MRP2, MRP3 and MRP4

2.4.1 Pilot Experiments

The fold changes for all eight statins evaluated at 1 and 10 µM and at two-time points (2 and 10 mins or 5 and 10 mins) are detailed in Table 3.4. For all three transporters, the probe $E_2$17βG was characterised by at least a 5-fold increase in accumulation (9.3 for MRP2, 28.6 for MRP3 and 5.8 for MRP4) in the presence of ATP against AMP. These data support the activity of the MRP2, MRP3 and MRP4 transport systems in vesicles.

Table 3.4. Fold increase in uptake of statins with MRP2, MRP3 and MRP4 with ATP compared to without ATP. Students t-test applied *P<0.05, **P<0.01, ***P<0.005 and ****P<0.0001. # incubation concentrations of $E_2$17βG 50 μM for MRP2, 1μM for MRP3 and 10 μM for MRP4.

Substrate		**MRP2 (min)**		**MRP3 (min)**		**MRP4 (min)**	
		2	**10**	**5**	**20**	**5**	**10**
Atorvastatin acid (μM)	1	1.05	0.948	1.41	0.886	1.06	1.81*
	10	0.820	1.31	1.61	1.26	1.34	1.53
Cerivastatin acid (μM)	1	0.971	0.470	1.05	1.29	1.67	0.828
	10	1.11	0.947	1.27	0.937	1.07	1.13
Fluvastatin acid (μM)	1	1.36	1.22	1.14	0.80	2.38****	1.47
	10	0.947	0.970	1.64	1.07	2.07****	1.78*
Lovastatin acid (μM)	1	0.752	1.45	ND	ND	1.10	0.220
	10	0.987	1.22	1.41	1.07	1.17	1.04
Pitavastatin acid (μM)	1	1.02	1.01	1.13	0.738	1.68	2.22***
	10	1.52	1.17	1.26	1.08	1.83*	2.49**
Pravastatin acid (μM)	1	0.963	1.21	1.81	2.59**	1.14	1.06
	10	0.721	1.37	7.06**	5.07**	1.21	1.12
Rosuvastatin acid (μM)	1	0.708	1.010	1.44	0.88	1.80*	1.63
	10	1.64	2.40**	1.55	1.88***	2.29**	1.95*
Simvastatin acid (μM)	1	0.261	0.788	0.600	1.16	1.67	1.04
	10	1.312	1.031	0.969	0.959	1.23	1.31
$E_2$17βG (μM)	#	Not conducted	9.3**	Not conducted	28.6****	Not conducted	5.8****

2.4.2 Uptake of Statins by MRP2

Uptake of atorvastatin, fluvastatin, lovastatin, pitavastatin, pravastatin and rosuvastatin was observed against MRP2. Although the ratios of ATP: AMP were >1, these ratios were less than 2-fold and not found to be statistically significant ($P<0.05$).

Only rosuvastatin yielded a positive result with a 2.40:1 ratio of uptake on MRP2 at 10μM /10 mins. This result was statistically significant at $P<0.01$ (Students *t*-test). The uptake of each statin across MRP2 is illustrated in Appendix 14 (a, b and c).

2.4.3 Uptake of Statins by MRP3

Most statins showed evidence of uptake but generally these were not found be to statistically relevant. However, for rosuvastatin a 1.88-fold uptake at 10 μM/20 mins was measured with Students *t* -test value of $P<0.005$. For pravastatin, fold differences of 1.88 and 2.59 were noted at 1 μM (5 and 20min, respectively) and 7.05 and 5.07 at 10 μM (5 and 20 min, respectively), where $P<0.01$. Both rosuvastatin and pravastatin were considered potential substrates of MRP3. The uptake of each statin across MRP3 is illustrated in Appendix 15 (a, b and c).

2.4.4 Uptake of Statins by MRP4

Similar to MRP3, most statins showed evidence of uptake but again these were not found be to statistically relevant apart from fluvastatin, pitavastatin and rosuvastatin. For fluvastatin induced 2.38-fold ($P< 0.0001$) and 2.07-fold ($P<0.0001$) uptake at 1 μM (5 and 10 min, respectively). Pitavastatin elicited 2.22-fold ($P<0.005$) and 2.49-fold ($P<0.001$) uptake at 1 μM (5 and 10 min, respectively). In the case of rosuvastatin, statically relevant uptakes of 1.8-fold ($P<0.05$), 2.29-fold ($P<0.01$) and 1.95-fold ($P<0.05$) were determined at 1 μM/5 min, 1 μM/10 min and 10 μM/10 min incubation combinations, respectively. The uptake of each statin across MRP4 is illustrated in Appendix 16 (a, b and c).

2.4.4.1 Time Dependence Experiments.

Of the time dependence experiments performed, only pravastatin with respect to MRP3 could be reported as illustrated in Appendix 17. Here transport was linear up to 5 mins. For all other combinations insufficient uptake was observed to enable a time course to be plotted.

2.4.5 Determination of Km for Pravastatin.

Individual and mean plots for the concentration dependent uptake of pravastatin by MRP3 are shown in Appendix 17. Calculation of concentration-dependent uptake was carried out for pravastatin on MRP3 at 2.5 mins to derive a Km and Vmax of 51.9 ± 10.8 μM and 51.3 ± 4.93 pmol/mg/min, respectively.

2.5 Statins as Inhibitors of Human MRP2, MRP3 and MRP4

The inhibitory effects of statins with respect to MRP2 and MRP3 were investigated by incubation with the known fluorescent probe substrate (CDCF). For MRP4, the probe substrate was $E_2$17βg measured by LC-MS/MS. The IC_{50} values for all statins against MRP2, MRP3 and MRP4 are shown in Table 3.5.

.

Table 3.5. IC_{50} values for the inhibition of 5μM CDCF uptake in to human MRP2 and MRP3 vesicles and 10 μM $E_2$17βg uptake in human MRP4 vesicles by statins. ND: IC_{50} values could not be determined

Statin/Positive Control	**MRP2 IC_{50} (μM)**	**MRP3 IC_{50} (μM)**	**MRP4 IC_{50} (μM)**
Atorvastatin	90.9 ± 6.30	2.30 ± 0.838	37.8 ± 4.69
Atorvastatin repeat	N/A	2.79 ± 0.327	N/A
Cerivastatin	220 ± 14.4	33.3 ± 6.45	31.9 ± 2.00
Fluvastatin	197 ± 21.5	14.3 ± 2.62	54.2 ± 8.35
Lovastatin	ND	13.9 ± 1.87	63.6 ± 13.2
Rosuvastatin	298 ± 23.7	18.8 ± 1.92	31.4 ± 5.74
Simvastatin	371 ± 61.2	15.9 ± 2.19	54.4 ± 5.53
Pitavastatin	135 ± 9.66	35.2 ± 29.3	29.3 ± 2.42
Pravastatin	ND	33.9 ± 11.2	245 ± 47.3
Benzbromarone	21.7 ± 1.44	25.1 ± 1.19	N/A
MK571	N/A	N/A	14.6 ± 3.28

2.5.1 Inhibition of CDCF Uptake by Statins Via MRP2 Vesicles

The inhibitory effects of statins and the probe inhibitor benzbromarone (BB) on MRP2 are summarised in Appendix 18 (a, b and c.) Benzbromarone inhibited the transport of 5 μM CDCF with a calculated of IC_{50} 21.7 ± 1.44 μM. Lovastatin and pravastatin showed no inhibition up to the 300 μM tested. All other statins were characterised as weak inhibitors with IC_{50} values above 90 μM (atorvastatin 90.9 ± 6.30 μM, cerivastatin 220 ± 14.4 μM, fluvastatin 197 ± 21.5 μM, rosuvastatin 298 ± 23.7 μM, pitavastatin 135 ± 9.66 μM and simvastatin 371 ± 61.2 μM)

2.5.2 Inhibition of CDCF Uptake by Statins Via MRP3 Vesicles

The inhibitory effects of statins and the probe inhibitor benzbromarone (BB) on MRP3 are summarised in Appendix 19 (a, b and c). Benzbromarone inhibited the transport of 5 μM CDCF with a calculated IC_{50} of 25.1 ± 1.44 μM. The IC_{50} determined for cerivastatin (33.3 ± 6.45 μM), fluvastatin (14.3 ± 2.62 μM), lovastatin (13.9 ± 1.87 μM), rosuvastatin (18.8 ± 1.92 μM), pitavastatin (35.2 ± 29.3 μM), pravastatin (33.9 ± 11.2 μM) and simvastatin (15.9 ± 2.19 μM) were similar to that observed for the BB. Atorvastatin was identified as a strong inhibitor of CDCF uptake with a calculated IC_{50} 2.30 ± 0.848 μM. This result was confirmed with an IC_{50} of 2.79 ± 0.327 μM following a repeat of this experiment with additional concentrations over the 0.04 to 300 μM range.

2.5.3 Inhibition of $E_2$17βg uptake by statins via MRP4 vesicles

For MRP4 the inhibitory effects of statins and the probe inhibitor MK571 are summarised in Appendix 20 (a, b and c). MK571 inhibited the transport of 10 μM $E_2$17βg, with a calculated IC_{50} of 14.6 ± 3.28 μM. All statins except for pravastatin (IC_{50} 245 μM) were shown to be moderate inhibitors (atorvastatin: 37.8 ± 4.69 μM, cerivastatin: 31.9 ± 2.0 μM, fluvastatin: 54.2 ± 8.35 μM, lovastatin: 63.6 ± 13.2 μM, rosuvastatin: 31.4 ± 5.74 μM, pitavastatin: 29.3 ± 2.42 μM and simvastatin: 54.4 ± 5.53 μM).

2.6 Utilisation of D300e Digital Dispenser

The D300e ability to dispense volumes ranging from pL to nL minimises the requirement of manual pipetting and preparation of serial dilutions. The intuitive software made it easy and extremely quick to generate plates for IC_{50} determinations and validation/calibration samples, reducing preparation times significantly from hours to minutes.

One important consideration to ensure effective mixing is that the stocks are delivered from the D300e onto a volume of incubate/solvent and not *vice versa* to ensure mixing.

3 Discussion

One of the aims of this project was to conduct all analytical measurements with non-radio-labelled substrates. Here I have demonstrated the quantitative determination of $E_2$17βg and several key statins can be achieved by means of LC-MS/MS. An LC-MS/MS approach has the advantages of no exposure to radioactive material, flexibility to run in any laboratory possessing LC-MS/MS hardware and reduction in costs for compounds. The measurements of $E_2$17βg as a probe substrate were conducted in under 20 mins and results could be assessed in a single day. With the implementation of the D300e digital dispenser, considerable time savings in sample preparation time were achieved.

3.1 Statins as Substrates for Transporters

The study of transport by these proteins was performed using inside-out orientated membrane vesicles in the presence of ATP. As ATP is required to actively transport a substrate, AMP was used as a negative control. High accumulation of a compound in vesicles in the presence of AMP is an indication that the compound is not a substrate and has passively diffused, which generally applies to compounds that are more hydrophobic and/or have high passive permeability. Another reason could be the substrate non-specifically binding to the vesicle, disguising transport.

3.1.1 Statins as Substrates for Human MRP2

Only rosuvastatin, was shown to be a substrate against MRP2 during the pilot assessments, with a 2.4-fold uptake observed in the presence of ATP over AMP. Although the fold accumulation was insufficient to define the kinetic parameters, these data are supportive of other published findings that rosuvastatin is a substrate for rat MRP2. Hobbs *et al* [79] established MRP2 and BCRP to be the major route of biliary efflux of rosuvastatin in an

isolated perfused rat liver (IPRL) model. Other models utilising sandwich cultured rat hepatocytes (SCRH) [80-82] and Mrp2-deficient rats (also referred to as Eisai hyperbilirubinemia rats) drew the same conclusions, where a decrease in the efflux of rosuvastatin was observed compared with wild type animals.

With respect to other statins, some evidence of ATP-dependent transport was observed for atorvastatin, fluvastatin, lovastatin, pitavastatin and pravastatin against MRP2. However, these values were lower than the acceptance criteria of 2-fold to define active transport uptake and no statistical value (Students *t*-test) could be assigned to these data. Conversely, results from those of Ellis *et al* [35] who, utilising an ATPase assay format, reported evidence for most statins as substrates for MRP2. Their data was also confirmed by Lau *et al* 2006 [83] and Kivisto 2005 [84] who reported the contribution of biliary excretion for atorvastatin and pravastatin by MRP2. Unlike the vesicular assay used here, the results generated from the ATPase assay (utilised by Ellis *et al*) are not susceptible to permeable drugs diffusing back out of the vesicles. The measurement of uptake with the ATPase assay is indirectly measured from the release of a phosphate ion during hydrolysis of ATP to ADP while transporting the substrate across the cell membrane. Interestingly, Huang e*t al* [85] also found no significant ATP-dependent transport of rosuvastatin with inverted vesicle membranes transfected with MRP2, whilst informing of active transport of rosuvastatin by BCRP. However, for BCRP they demonstrated the effect of osmolarity on ATP- dependent transport by altering the concentration of sucrose in different incubations and therefore favouring the characterisation of the BCRP experimental conditions.

Further work would be required to fully understand the reasons for the discrepancies in my findings to those reported in literature (see section 3.2).

3.1.2 Statins as Substrates for Human MRP3

To date, statins as substrates for MRP3 have been studied far less than those of MRP2. Within this project pravastatin was identified to be a substrate for MRP3. A greater than 5-fold accumulation was measured from pilot experiments and subsequently confirmed with the determined of Km and Vmax values of 51.9 ± 10.8 μM and 51.3 ± 4.93 pmol/mg/min, respectively. Evidence for active transport of rosuvastatin by MRP3 was also observed, although the fold difference of ATP accumulation was less than 2-fold (1.88) between incubations with and without ATP. Although no kinetic parameters could be determined, statistical t-test ($P<0.005$) analysis suggests that the results are valid for active transport of rosuvastatin by MRP3. To our knowledge, this is the first study to report these findings for pravastatin and rosuvastatin. Under certain conditions, the affinity of pravastatin or rosuvastatin for MRP3 could be of importance as discussed below.

Biliary excretion accounts for ~34% and 70% of the elimination of unchanged pravastatin and rosuvastatin, respectively [86-88] for which MRP2 has been identified as contributing substantially [79, 84, 89]. Reduced biliary efflux of pravastatin has been demonstrated to increase its systemic exposure (2- to 6-fold) following intravenous infusion into Mrp2-deficient (TR^-) rats compared to wild type [84]. The lack of MRP2 due to a genetic defect in the ABCC2 encoding gene [48, 49, 90, 91] in humans is known as Dubin-Johnson Syndrome (DJS) [84, 88, 92]. Although not life-threatening, elevated levels of conjugated bilirubin arising from the break-down of haem, bring about the darkening of the liver or jaundice (yellowing skin pigmentation). It is noteworthy, that whilst the findings of Kivisto *et al* agree with these data, their study also found that the pharmacokinetic half-life $t_{½}$ was not reduced as much as expected in TR^- rats compared to wild type. Here they postulated that up-regulation of MRP3 could be a compensatory process for the clearance process of pravastatin. Konig *et al* have also highlighted overexpression of MRP3 in liver samples patients suffering

from Dubin-Johnson syndrome [93]. Up-regulation of Mrp3/MRP3 expression has also been observed in response to cholestasis due to increased concentrations of the bile salt chenodeoxycholic acid and bile duct ligation [94, 95]. In cases of obstructive cholestasis (as a consequence of gall stones blocking the bile ducts) these patients have elicited a 3.4-fold increase in MRP3 expression over of non-cholestatic patients [50].

For the reasons discussed, the impact of the observed transport for rosuvastatin and pravastatin by MRP3 could be greater in instances where MRP2 has been inhibited or impaired, although to date, the clinical relevance of this data is unknown.

3.1.3 Statins as Substrates for Human MRP4

The pilot data described in this thesis showed evidence of atorvastatin, fluvastatin and pitavastatin as potential substrates for MRP4. Data published by Pfeifer et al. 2013 [33] corroborates the findings presented here for the case of rosuvastatin. Uptake was observed following concentration-time experiments for these three statins, but the extent of uptake was insufficient to plot a suitable course. Expression of MRP4 in the liver is known to be significantly lower than for both MRP2 and MRP3 [96, 97], but can also be upregulated [52, 97], which could be of clinical relevance. However, the relevance to clinical studies is yet unknown and therefore may warrant further consideration. Expression of MRP4 is also present in the sarcolemma of human skeletal muscle. Thus, in addition to transport by OATP2B1, uptake in the muscle of these statins shown to be substrates for MRP4 may also contribute to myopathy.

3.2 Further observations and Discussion

Reasons for the discrepancies in the MRP2 data reported here in this thesis to that in literature could be due to non-specific binding effects of the statins to the vesicle membranes or apparatus. This would result in a higher background in the control (AMP) samples leading to

false negatives. No evidence for a significant non-specific binding effect were observed during the assay validation (3.2.3), although assessments of non-specific binding were not performed for all statins. Arguably, for those statins studied, the experiments were not conducted in the presence of AMP and ATP (assay buffer only with mock vesicles), however as both solutions are adjusted to pH 7 this is not considered to be a contributing factor.

Regardless of their lipophilicities, back-ground levels of all statins were detected in AMP incubations, most likely due to passive permeability. The pilot studies involved only semi-quantitative analyses and as consequence of different MS responses for each statin, it is not possible to deduce any correlation with respect their physiochemical properties. This could be investigated with radiolabelled statins.

Due to the number of statins being evaluated herein and the cost of vesicles, assessments were only performed under limited situations (2-time points (fast and slow), 2 concentrations (low and high)). Nevertheless, these experiments indicate whether a statin was a substrate for a particular MRP transporter and assist in the further experimental design for kinetic analysis. As fold accumulations ranging from 5.8 to 28.6 were determined for the probe controls across the different transporters, then the data reported here are valid (under these conditions). Noteworthy is that both passive and active transport *in vivo* play important roles in defining absolute concentrations of drugs crossing cellular barriers [98].

Interestingly, the statins that showed ATP-dependent uptake were generally hydrophilic in nature (logD) e.g MRP2, 3, 4 vs rosuvastatin (-0.24), MRP3 vs pravastatin (-0.88), pitavastatin (-1.2), with the exception of fluvastatin (+1.34) with MRP4.

For improved characterisation, additional timepoints and concentrations could have been assessed or further factors in the incubation environment evaluated, such as sensitivity to osmolarity, which affects the intra-vesicular space and in turn the permeability of substrates.

Mock vesicles lacking the expressed transporter could have been used as negative controls instead of AMP. If the accumulation is similar in both, then an endogenous transporter is probably responsible. However, the expense of mock vesicles meant the decision was taken to use AMP as a negative control. Ideally as confirmation of uptake results, experiments would be conducted again with mock vesicles.

Overall, there was no class effect observed for statins with respect to being substrates for MRP2, MRP3 or MRP4, although these data suggest that the hydrophilic statins are more likely to be actively transported.

3.3 Statins as Inhibitors of Human MRP2, MRP3 and MRP4

The consequence of inhibiting transporters is of significant interest and importance. Just as the inhibition of metabolising enzymes can greatly affect the efficacy and safety profile of a drug, so holds parallel for transporters. These two mechanisms (metabolism and transport) need to be considered in conjunction. For example, rhabdomyolysis was observed following the co-administration of simvastatin with the antibiotic ciprofloxacin. As an CYP3A4 inhibitor, ciprofloxacin inhibits the metabolism of simvastatin, increasing its circulating concentrations and subsequently its myotoxicity [99]. The uptake of statins into the liver (their site of action) is also largely dependent on active transport by OATP1B1 and OATPIB3. When co-administered with inhibitors of OATP1B1 (e.g. gemfibrozil or rifampicin) then an increase in the circulating plasma concentrations of statins is observed [32].

Drugs can act as both victims and perpetrators of drug-drug interactions. Inhibition of statin transport has been reported widely [24, 100-103] whereas data around statins as potential inhibitors is limited to Pgp and MRP2 [35, 104, 105]. Explored here is the possible impact of statins as inhibitors of MRP2, MRP3 and MRP4.

All statins showed inhibitory effects against at least one of the MRPs. Against human MRP2, IC_{50} values of >100 µM were observed for all statins, except lovastatin and pravastatin where no inhibition of the uptake of CDCF was observed, even at concentrations of 300 µM. These data are in general in agreement with those reported by Chen *et al.*, who showed utilising Madin-Darby canine Kidney cells expressing MRP2 that the acidic forms of statins inhibited the uptake of MRP2 at IC_{50} values >100 µM [30]. However, there are conflicting findings for lovastatin acid. Chen *et al.* reported an IC_{50} >33 µM for lovastatin against MRP2, but observed no inhibition of CDCF uptake for concentrations up to 300 µM in these experiments. Furthermore, lovastatin appeared to be an inhibitor of MRP2 in a similar vesicle-based assay where Ellis and co-workers also reported IC_{50} values <25 µM for all statins tested [35] (although the concentration of CDCF was 5-fold lower (1 µM). This difference in substrate concentration could explain the disparity in the results published.

To date, there is a sparsity of literature examples concerning the potential inhibitory effects of statins with respect to MRP2, MRP3 and MRP4. Here we have shown that 6 out of 7 statins (simvastatin lactone the exception) inhibited MRP3-mediated transport while 6 out of 7 statins (pravastatin the exception) inhibited MRP4. For those statins identified as inhibitors of MRP3 and MRP4, the probe substrate IC_{50} values ranged from 64 µM down to 1.68 µM.

These data could be of clinical significance in patients with impaired MRP2 function or reduced protein expression but with upregulated MRP3 and MRP4 as a compensation mechanism. Administration of statins under these circumstances, especially atorvastatin (IC_{50} of 1.68 µM against MRP3) could theoretically exacerbate any hyperbilirubinemia.

Interestingly, there are several studies that suggest atorvastatin could be associated with liver damage [106, 107]. Clarke *et al* [108] reviewed 7 individual case studies, where patients on co-medication with prescribed atorvastatin subsequently developed liver abnormalities (such

as significant bilirubin levels and non-specific cholestasis). In most instances, liver functions normalised following discontinuation of atorvastatin, although 3 patients were hospitalised, and one death was recorded. Whilst other statins were also suspected of hepatotoxicity, the increased risk observed for atorvastatin was attributed to its longer exposure [109].

Intriguingly for a couple of cases that Clarke *et al* studied, patients were prescribed ramipril for hypertension. Following de-esterification, the major route of clearance of ramipril is *via* glurconidation with subsequent elimination of this metabolite through biliary excretion. MRP3 substrate specificity is similar to that of MRP2 (organic anions such as glucuronide and sulphate conjugates) [77]. Here I postulate that atorvastatin could also be inhibiting efflux of ramipril glucuronide by MRP2 or MRP3 and in turn contributing to their liver dysfunction.

Szabo and co-workers-[110] explored the hypothesis that statins could cause liver impairment, characterised by increased levels of bilirubin. They investigated the biliary efflux of bilirubin in the presence of several statins (including atorvastatin) using sandwich-cultured rat hepatocytes. Their observations were not supportive of the hypothesis as they found that statins both inhibited and stimulated MRP2 and MRP3, thus not affecting the overall levels of intracellular bilirubin. It is important to note, however, bile salt conjugates (particularly sulphates) have also been determined as substrates for MRP3 [111] and therefore inhibition of their efflux by this transporter could be another explanation of liver impairment.

Just as MRP3 is known for transport of endogenous conjugates, awareness is growing of its ability to transport glucuronide and sulphate drug metabolites. The disposition of the metabolites such as morphine-3-glucuronide, morphine-6-glucuronide and paracetamol glucuronide have all been shown to be altered in mice lacking the Mrp3 gene [112, 113].

Both MRP3 and MRP4 are involved in the transport of endogenous folates required for cell division and the drug analogue methotrexate (MTX), which is both used widely as an anti-inflammatory agent and chemotherapeutic is also a substrate [44, 114]. Vlaming *et al* observed similar findings with knock out mice (Abcc3^{-}) and advised care when methotrexate is co-administered with known MRP3 inhibitors.

Understanding the impact of MRP2, MRP3 and MRP4 inhibition is in its infancy and requires further characterisation. Inclusion of the inhibitory characteristics of these transporters in physiologically-based pharmacokinetic (PBPK) models would refine the predictive power of these models and aid in the assessment of drug-drug interactions at the level of the hepatocyte. Furthermore, this would provide a more holistic understanding of the overall effect of the MRP transporters with respect to statin disposition.

Vesicles preparations are a clean system relative to other model *in vitro* systems. They allow the transport characteristics to be assessed for each statin/transporter pair in the absence of competing effects. However, to understand the ultimate interplay (transporter to transporter, transporter to enzyme) and the effect statins may have on the disposition of a drug, then a more mechanistic model would be required, such as sandwich-cultured rat hepatocytes or knockout mice models.

3.4 Correlation of Uptake and Inhibition data

The determination of Km or IC_{50} are both assessments of the affinity of a substrate for a target transporter, whether it binds competitively or non-competitively. It should not be surprising that when pulled together there are correlations between the uptake and inhibition experimental data. In the case of MRP2, statins overall appeared to have a low affinity with little uptake observed. This is supported by IC_{50} values > 90 for all statins, indicating a low affinity for competitive or non-competitive inhibition.

IC_{50} values for statins pertaining to MRP3 and MRP4 are significantly lower than those against MRP2. For both these MRPs there is more evidence of the affinity of statins for them as substrate compared to MRP2. For pravastatin this is nicely illustrated by the similar Km and IC_{50} values of 51.9 μM and 33.9 μM, respectively.

4 Summary and Conclusions

Understanding the clinical importance of basolateral hepatic transporters with respect to their contribution to drug disposition is an emerging area. In summary, I have shown that MRP2, MRP3 and MRP4 can potentially influence the disposition of certain statins:

The following statins were identified as substrates for the different protein transporters

MRP2: Rosuvastatin

MRP3: Pravastatin, rosuvastatin

MRP4: Fluvastatin, pitavastatin, pravastatin

Moreover, certain statins may also inhibit MRPs;

MRP2: All statins (weak inhibitors except for lovastatin)

MRP3: All statins moderate to strong inhibitors especially atorvastatin

MRP4: All moderate inhibitors except pravastatin (weak)

The implications of statins as perpetrators of MRP3 and MRP4 inhibition may be of more clinical relevance than their behaviour as substrates. Because statins are widely prescribed, caution should be taken in cases of impaired MRP2, either by disease (cholestatic) or genetic disorders/polymorphisms and in cases when co-administered with drugs whose disposition is affected by MRP3 transport (methotrexate, morphine). Under these circumstances (especially when administering atorvastatin), changes in the bile acids could be monitored, and any possible interactions could be averted by altering the dose or changing statin.

There is an increasing interest from regulators to understand the disposition of metabolites, and hepatic efflux has been shown to play a key role in the clearance of conjugated metabolites. However, correlation of *in vitro* data to *in vivo* models still needs to be fully understood and the relationship to clinical settings.

5 APPENDICES

Appendix 1: Schematic of the methodology utilising ultrafiltration for sample preparation and the measurement of uptake in MRP2, MRP3 and MRP4 via LC-MS/MS or Fluorescence.

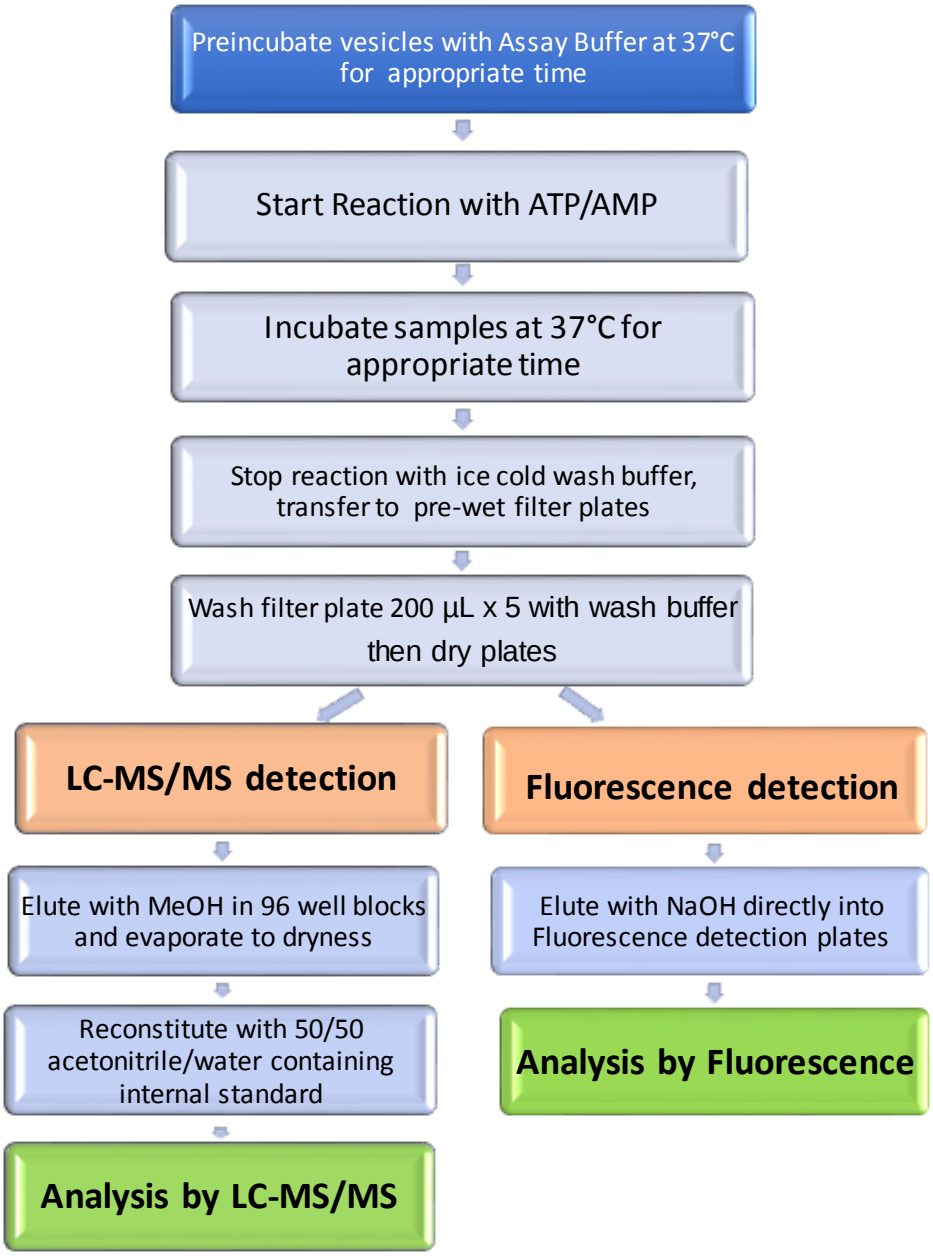

Appendix 2: The key mass spectrometer parameters of all analytes quantified by LC/MS/MS with the time a chromatographic peak for each was observed (retention time). The molecular mass of each analyte monitored – 1H is depict as the Q1 value and following fragmentation of these ions the most sensitive responding product ion detected is listed as Q3 with its corresponding collision energy applied to achieved.

Mass spectrometer Make/Model	AB SICEX API5000
Ionisation interface	TurboIonSpray
Mode	Negative ion
Ionspray voltage	-2500 V
Ion source Gas 1	30 psi
Ion source Gas 2	50 psi
Curtain Gas	35 psi

Analyte	**Q1 (m/z)**	**Q3 (m/z)**	**Declustering Potential**	**Collision Energy**	**Retention time (min)**
Rosuvastatin	480.3	418.3	-104	-21	0.80
Atorvastatin	557.4	278.2	-104	-30	1.10
Fluvastatin	410.3	348.2	-104	-21	1.16
Cerivastatin	458.4	396.3	-104	-23	1.40
Pitavastatin	420.3	358.2	-104	-18	1.02
Pravastatin	423.3	321.1	-100	-22	0.60
Lovastatin	431.3	319.2	-84	-23	1.30
Simvastatin	435.3	319.2	-100	-24	1.38
$E_2$17βG	447.3	113.2	-130	-35	0.75
DHEAS	367.3	97.2	-100	-49	0.92
I.S (Generic)	429.1	200.2	-100	-35	1.2

Appendix 3: HPLC conditions for the analysis of statins, $E_2$17Bg and DHEAS. The first half of the table describes the autosampler and analytical column used with the associated settings and conditions. The chromatographic gradient condition used for all analytes are shown in the second table.

Autosampler	Waters Acquity
Injector Wash Solvent 1 Strong Solvent Wash	1500 µL 40:30:30 acetonitrile:isopropanol:water +0.1% formic acid
Injector Wash Solvent 2 Weak Solvent Wash	900 µL 20:80 acetonitrile:water
Typical Injection Volume	5 µL
Sample Loop Option	Partial Loop
Load Ahead	Enabled
Loop Offline	Disabled, 0.2 minutes
Chromatography System	Waters Acquity UHPLC
Flow Rate	0.8 mL/min
Analytical Column	Waters Acquity, BEH C18, 50 x 2.1mm i.d. BEH C18 1,7 µm,
Column Temperature	40°C
Column Divert	Eluent from the column was diverted from the mass spectrometer between 0 and 0.6 min
Run Time	1.8 minutes
Mobile Phase A	5 mM ammonium bicarbonate (native pH)
Mobile Phase B	Acetonitrile

Gradient conditions		
Time (Min)	% Solvent A	% Solvent B
0	95	5
0.2	95	5
1.2	30	70
1.6	5	95
1.61	95	5

Appendix 4. 5mM analytical standards (A) for each statin and $E_2$17βg were prepared in DMSO. The preparation of working solutions (A1 to A5) are shown below and the subsequent dilutions for calibration standards.

Working Solution	**Statin/ $E_2$17βg**	**Dilution factor**	**Volume of 10 mM Stock (µL)**	**Volume of Internal Standard (µL)**	**Final Concentration (mM)**
A1	Rosuvastatin	X 50	20µL of each	900	0.1
	Pitavastatin				
	Pravastatin				
	Fluvastatin				
	$E_2$17βg				

Working Solution	**Volume of Working Solution**	**Volume of Internal Standard solution (µL)**	**Concentration (µM)**
			$E_2$17βg /STATIN
A2	100 µL of A1	900	10
A3	100 µL of A2	900	1
A4	100 µL of A3	900	0.1
A5	100 µL A4	900	0.001

Concentration of Statins/ $E_2$17βg (nM)	Volume of Spiking Solution (µL)					Volume of I.S Solution (µL)
	A5	A4	A3	A2	A1	
0.1	10					990
0.5	50					950
1		10				990
2.5		25				975
5		50				950
50			50			950
100				10		990
250				25		975
800					8	992
1000					10	995

Appendix 5. Matrix Effects on The Mass Spectrometer Peak Area Response (Statin response/internal standard response) for Rosuvastatin, Fluvastatin, Pitvastatin, Pravastatin and $E_2$17βg. The effect of matrix was assessed at a low and high concentration.

	Fluvastatin		**Pitavastatin**		**Pravastatin**		**Rosuvastatin**	
Concentration	**No Matrix**	**Matrix**	**No Matrix**	**Matrix**	**No Matrix**	**Matrix**	**No Matrix**	**Matrix**
0.5 nM	6192	10519	4600	5859	4848	5408	2470	2168
	5136	8647	3418	4867	4055	4994	2346	2122
	5050	10021	3642	5163	4472	4898	2268	1972
	4860	10307	3799	5670	4453	4886	2000	2147
	5568	10792	3868	5837	4536	5912	1979	2032
	5349	8777	3850	4297	4102	IS	1912	IS
Mean	5359	9844	3863	5282	4411	5220	2163	2088
SD	476	913	399	624	295	442	229	83
%CV	**8.9**	**9.3**	**10.3**	**11.8**	**6.7**	**8.5**	**10.6**	**4.0**
% Effect of matrix	**45.6**		**26.9**		**15.5**		**-3.6**	

IS = Insufficient sample

	Fluvastatin		**Pitavastatin**		**Pravastatin**		**Rosuvastatin**	
Concentration	**No Matrix**	**Matrix**	**No Matrix**	**Matrix**	**No Matrix**	**Matrix**	**No Matrix**	**Matrix**
200 nM	2441832	3699514	1597032	1798725	1781105	1941825	916462	938529
	2561501	3869192	1665703	2207584	1902509	2122184	976696	954122
	2413211	4100648	1553474	2411466	1782121	2535659	908795	1006276
	2480403	3129404	1596219	1942826	1803837	1919995	925353	923893
	2443793	3728966	1573995	2103184	1782485	2042295	918784	937987
	2442385	3322211	1564294	1915623	1831700	1970813	931415	996290
Mean	2468259	3641656	1591786	2063235	1813960	2088795	932208	959516
SD	57314	357173	40127	223585	47628	231075	26245	33885
%CV	2.3	9.8	2.5	10.8	2.6	11.1	2.8	3.5
% Effect of matrix	**32.2**		**22.8**		**13.2**		**2.85**	

Appendix 6. Back Calculated Calibration Standard Data and Associated Parameters for Rosuvastatin, Fluvastatin Pitavastatin, Pravastatin and $E_2$17βg

Analyte	*n*		STD 1	STD 2	STD 3	STD 4	STD 5	STD 6	STD 7	STD 8	*R*
Rosuvastatin	2	STD (nM)	0.25	0.50	1.00	5.00	10.0	50.0	125	250	0.9925
		% Accuracy	98.0	102.4	103.4	101.2	98.4	96.9	102.4	99.8	
		%CV	19.2	3.07	4.50	0.97	0.44	1.16	1.15	3.36	
Fluvastatin	2	STD (nM)	0.25	0.50	1.00	5.00	10.0	50.0	125	250	0.9935
		% Accuracy	100.4	98.7	101.1	101.7	100.3	99.7	99.7	100.4	
		%CV	7.64	10.7	8.22	1.84	2.10	2.63	0.98	2.42	
Pitavastatin	2	STD (nM)	0.25	0.50	1.00	5.00	10.0	50.0	125	250	0.9929
		% Accuracy	97.0	102.2	106.4	99.5	96.2	96.8	96.1	100.2	
		%CV	2.47	6.80	0.16	4.61	4.44	0.10	0.16	5.74	
Pravastatin	2	STD (nM)	0.25	0.50	1.00	5.00	10.0	50.0	125	250	0.9941
		% Accuracy	100.4	98.7	101.1	101.7	100.3	99.7	99.7	100.4	
		%CV	4.16	3.79	1.65	6.68	1.81	1.34	0.03	3.32	
$E_2$17βg	2	STD (nM)	1.00	2.5	5.0	50	100	250	800	1000	0.9940
		% Accuracy	100.2	94.8	111.8	104.7	101.7	100.2	92.2	93.5	
		%CV	2.38	2.95	2.17	1.14	13.9	1.78	2.12	7.45	

Appendix 7. Calibration Plot 0.25 -250nM and Chromatogram of the LLQ for Fluvastatin

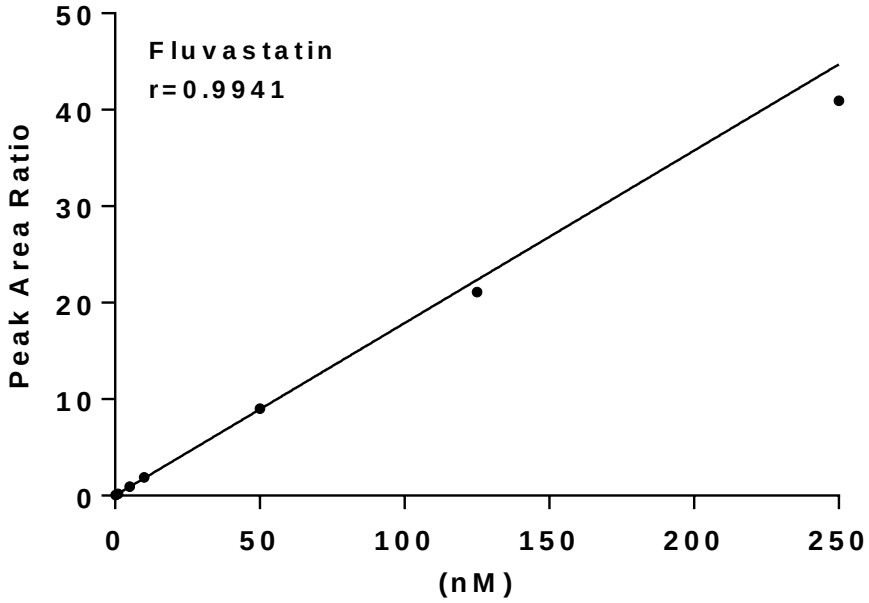

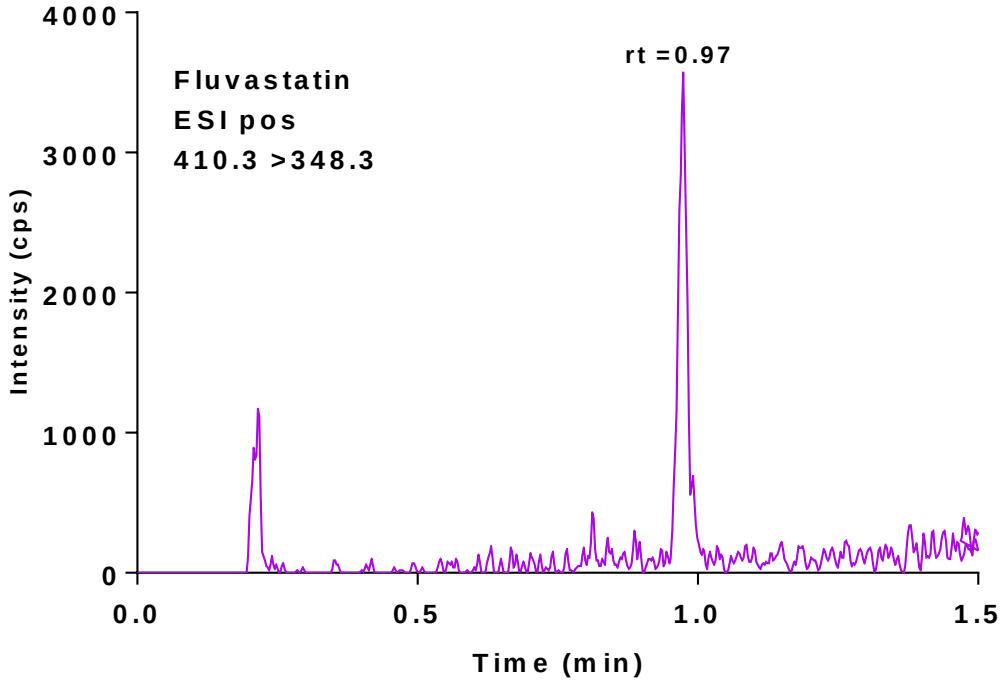

Appendix 8. Calibration Plot and Chromatogram of the LLQ for Pitavastatin

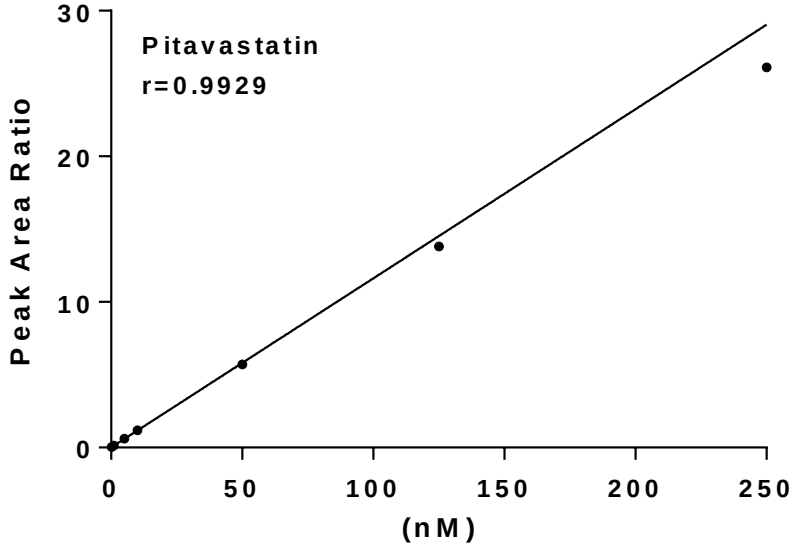

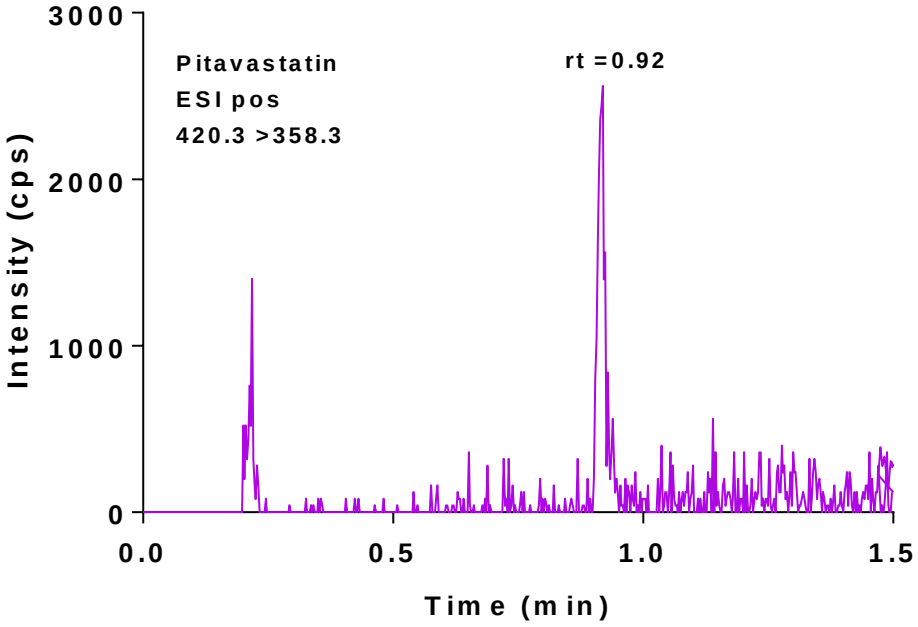

Appendix 9. Calibration Plot and Chromatogram of the LLQ for Pravastatin

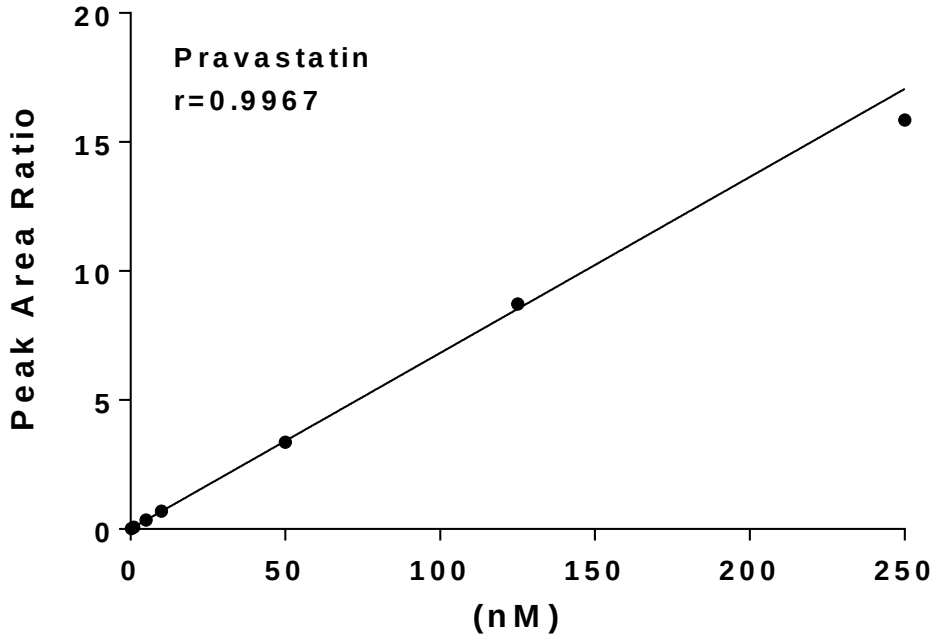

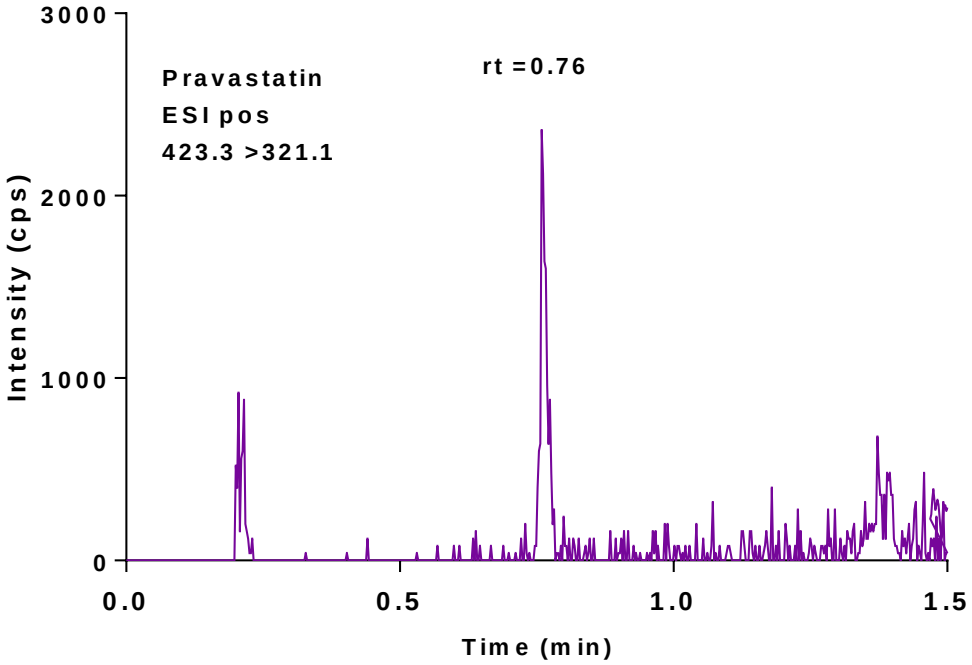

Appendix 10. Calibration Plot and Chromatogram of the LLQ for Rosuvastatin

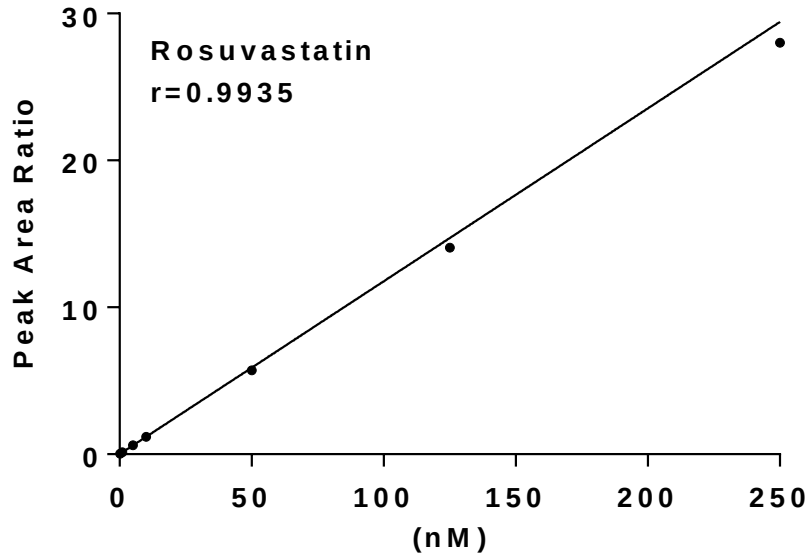

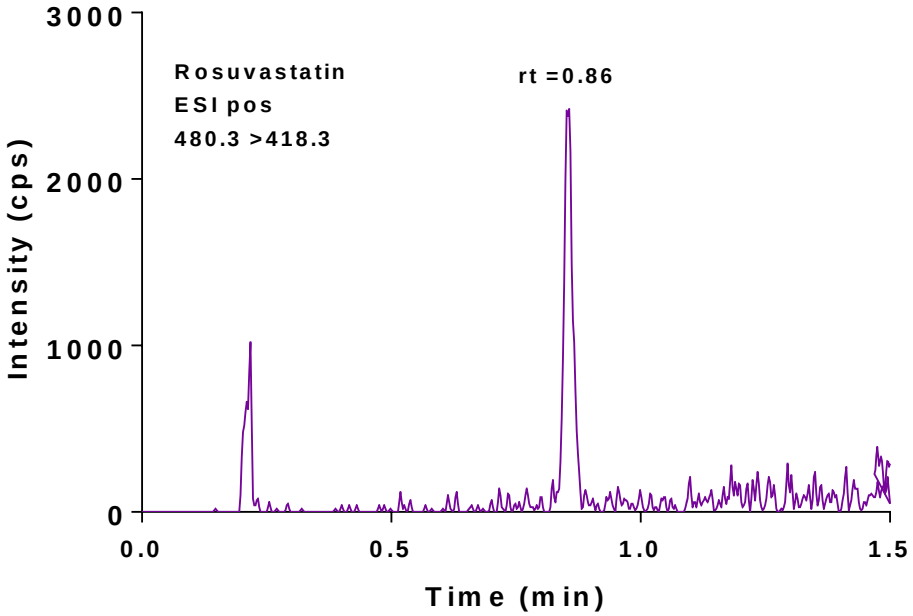

Appendix 11. Calibration Plot and Chromatogram of the LLQ for $E_2$17βg

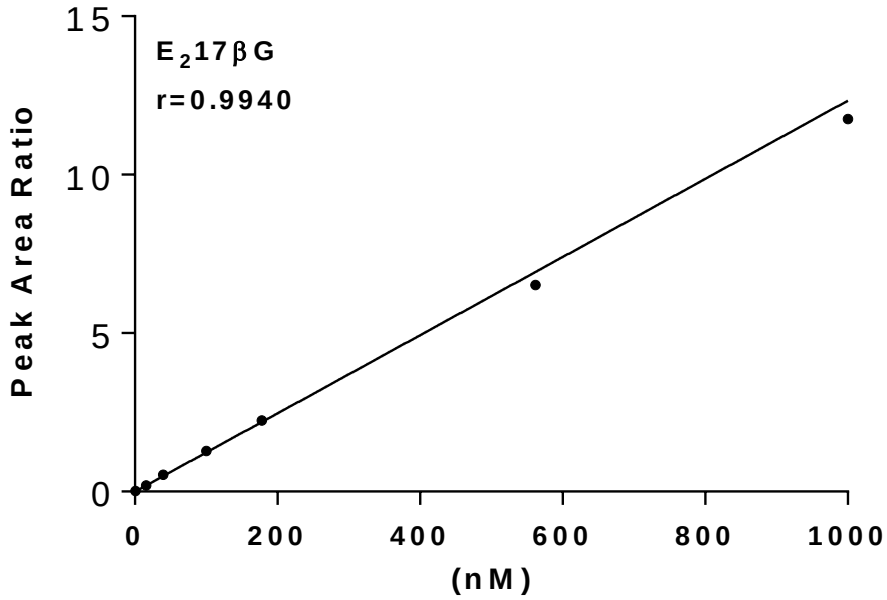

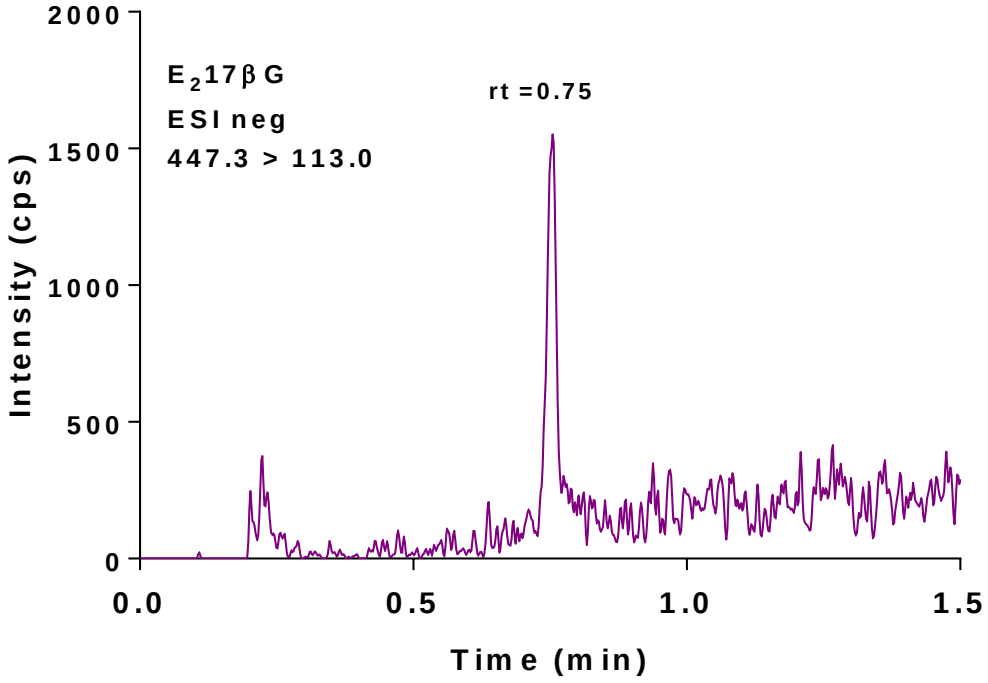

Appendix 12. Summary of Bias, Precision for Rosuvastatin, Fluvastatin, Pitavastatin, Pravastatin and $E_2$17βg in Extracted CTRL Vesicle Matrix

Analyte	***n***		**QC 1**	**QC 2**	**QC 3**	**QC 4**	**QC 5**
Rosuvastatin	6	QC (nM)	0.25	0.5	50	200	250
		% Accuracy	98.7	103.0	99.3	98.5	102.3
		%CV	9.59	6.47	2.47	1.47	4.54
Fluvastatin	6	QC (nM)	0.25	0.5	50	200	250
		% Accuracy	87.8	102.7	99.8	97.1	99.6
		%CV	7.41	5.38	2.92	1.80	3.01
Pitavastatin	6	QC (nM)	0.25	0.5	50	200	250
		% Accuracy	97.4	97.5	98.4	97.5	100.2
		%CV	5.62	4.78	2.60	0.87	5.31
Pravastatin	6	QC (nM)	0.25	0.5	50	200	250
		% Accuracy	88.8	95.7	99.8	97.6	97.9
		%CV	17.7	10.8	2.53	1.31	3.34
$E_2$17βg	6	QC (nM)	1.0	2.0	50	800	1000
		% Accuracy	89.8	101.9	100.7	88.1	110.9
		%CV	6.70	4.34	11.4	5.78	8.01

Appendix 13. Stability Data for E217βg in Assay Buffer at 37°C for 30 min

	Conc 1 µM Response		Conc 50 µM Response	
	T= 0	T= 30	T= 0	T= 30
Rep 1	3681	3819	215859	199169
Rep 2	3778	3629	201792	191939
Rep 3	3873	3653	199738	213053
Rep 4	3998	3308	209120	206402
Rep 5	3705	3725	194467	199639
Rep 6	3355	3942	202268	197142
Mean	**3742**	**3652**	**201477**	**201635**
SD	**242**	**228**	**5275**	**8235**
%CV	6.5	6.2	2.6	4.1
% Difference	-2.47		0.08	

Appendix 14a.: Uptake of Statins on human MRP2 vesicles with 1 or 10 µM of (A) atorvastatin, (B) cerivastatin and (C)fluvastatin incubated at 2 and 10 minutes of incubation. Students t-test applied *P<0.05, **P<0.01, ***P<0.005 and ****P<0.0001

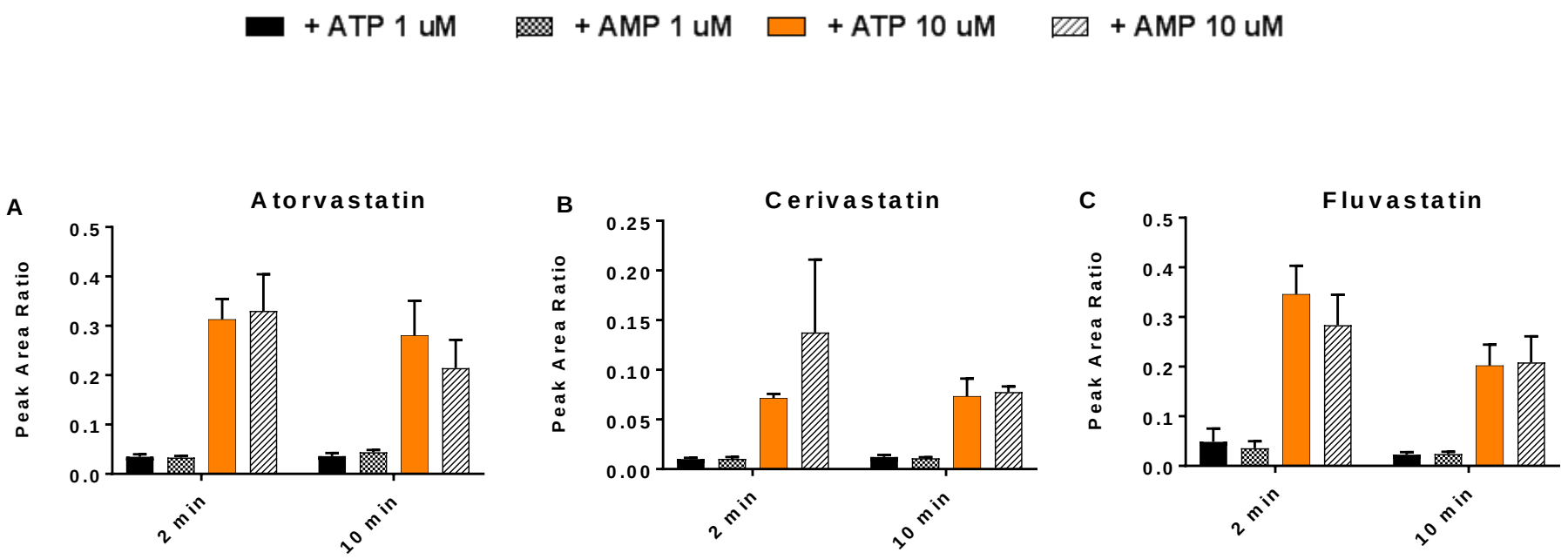

Appendix 14b.: Uptake of Statins on human MRP2 vesicles with 1 or 10 µM of (D)lovastatin, (E) pitavastatin, and (F) pravastatin at 2 and 10 minutes incubation. Students t-test applied *P<0.05, **P<0.01, ***P<0.005 and ****P<0.0001

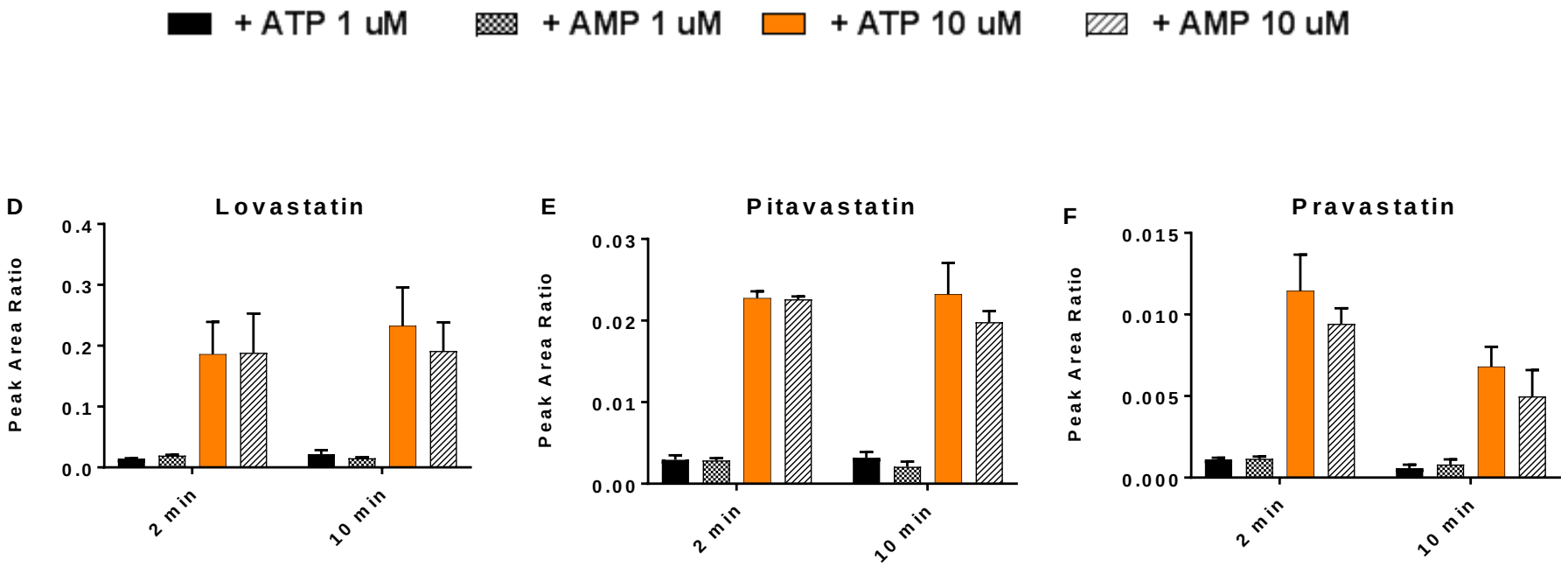

Appendix 14c.: Uptake of Statins on human MRP2 vesicles with 1 or 10 µM (G)rosuvastatin, (H) Simvastatin at 2 and 10 minutes of incubations and (I) Positive control $E_2$17βG at 50 µM with 10 minutes of incubation. Students t-test applied *P<0.05, **P<0.01, ***P<0.005 and ****P<0.0001

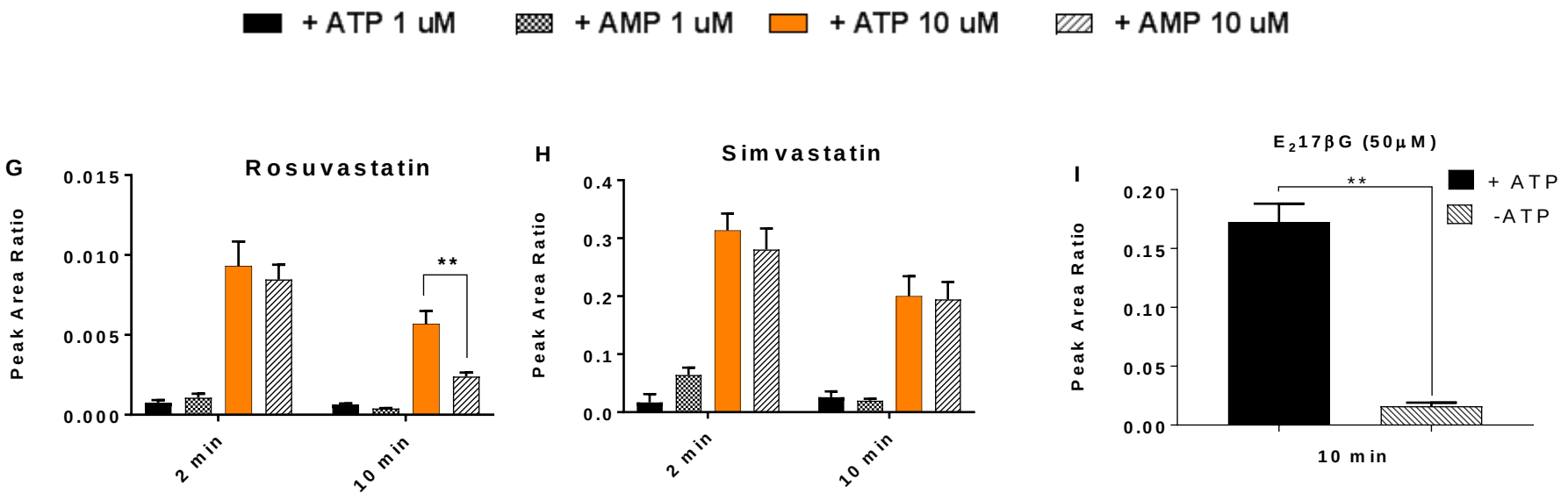

o

Appendix 15a.: Uptake of Statins on human MRP3 vesicles with 1 or 10 µM of (A) atorvastatin, (B) cerivastatin and (C)fluvastatin incubated at 5 and 20 minutes of incubation. Students t-test applied *P<0.05, **P<0.01, ***P<0.005 and ****P<0.0001

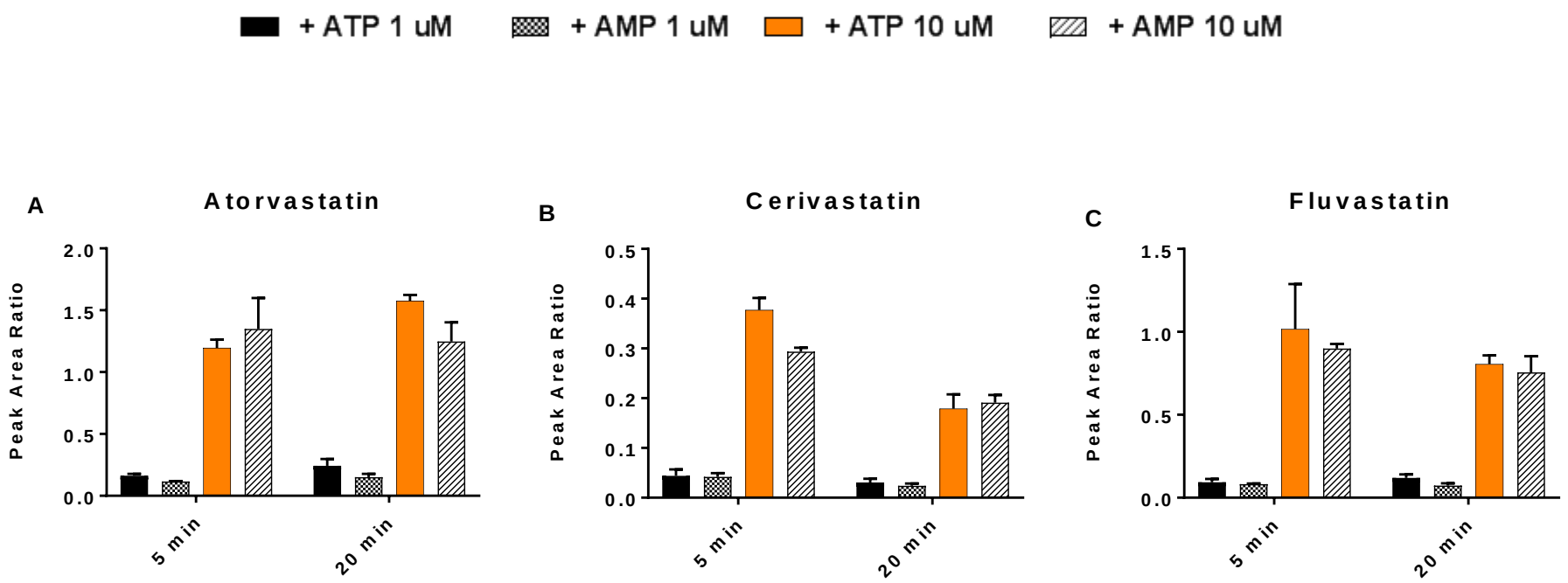

Appendix 15b.: Uptake of Statins on human MRP3 vesicles with 1 or 10 μM of (D)lovastatin, (E)pitavastatin, and (F) pravastatin at 5 and 20 minutes incubation. Students t-test applied *P<0.05, **P<0.01, ***P<0.005 and ****P<0.0001

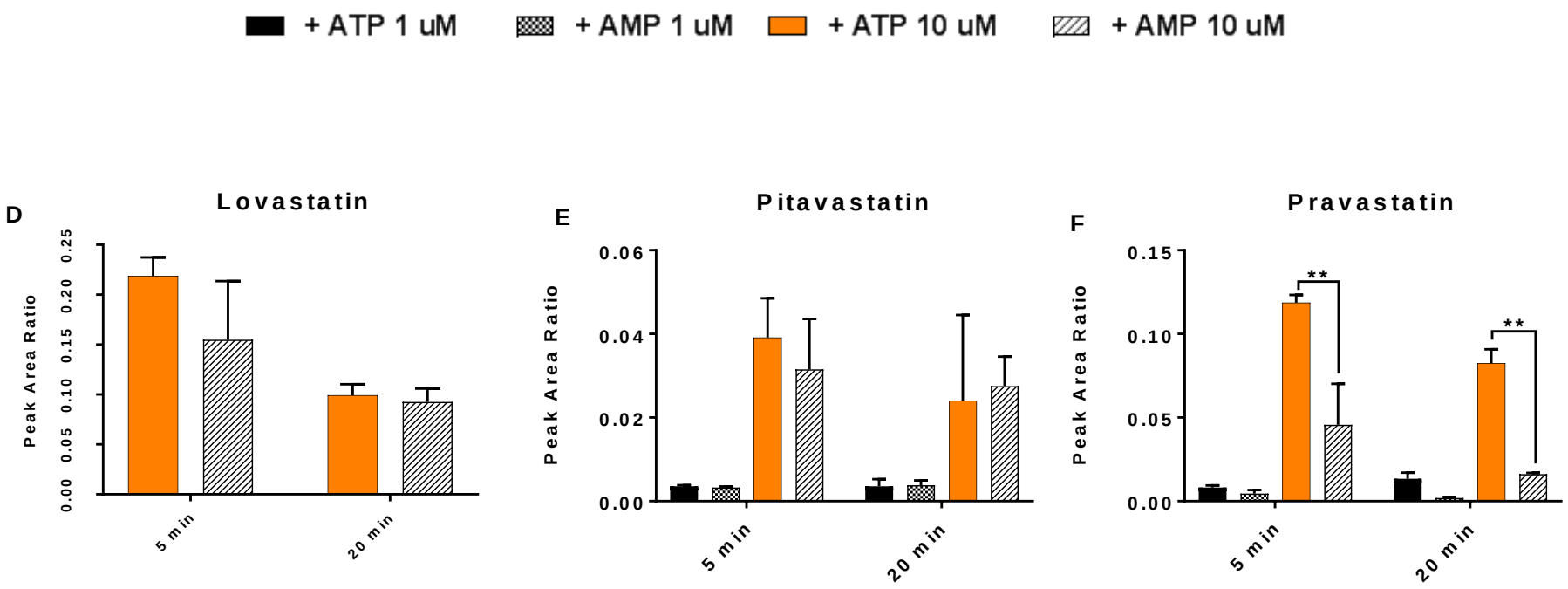

Appendix 15c.: Uptake of Statins on human MRP3 vesicles with 1 or 10 µM (G)rosuvastatin, (H) Simvastatin at 5 and 20 minutes of incubations and (I) Positive control $E_2$17βg at 1 µM with 10 minutes of incubation. Students t-test applied *P<0.05, **P<0.01, ***P<0.005 and ****P<0.0001

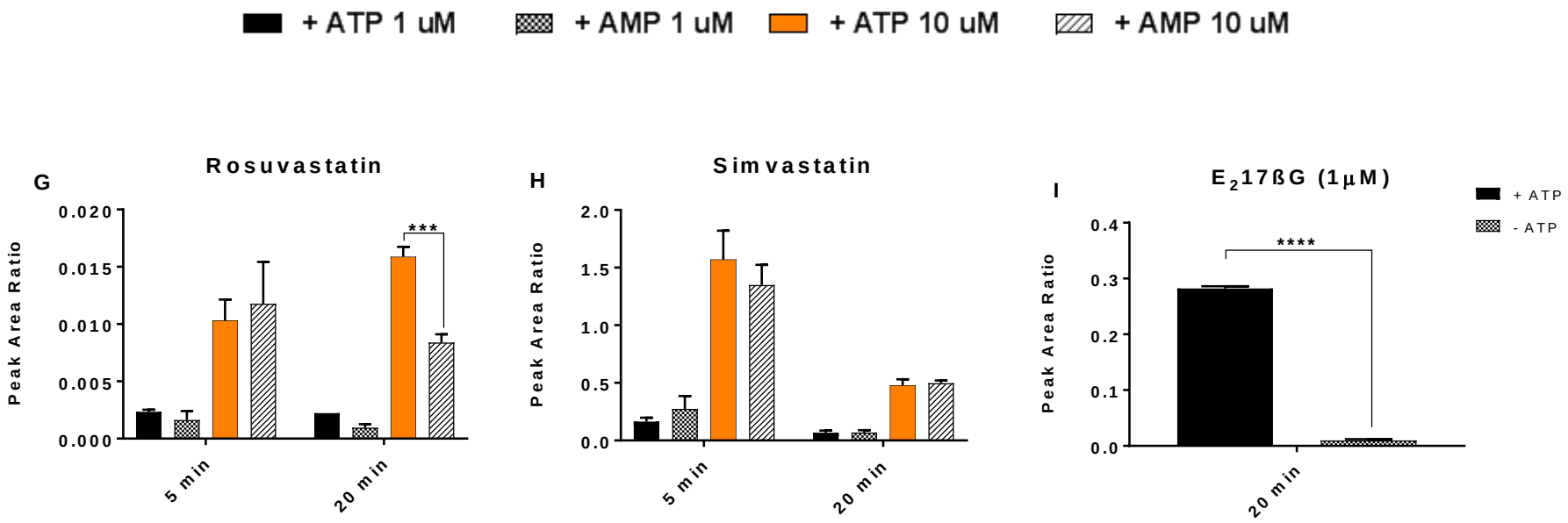

Appendix 16a.: Uptake of Statins on human MRP4 vesicles with 1 or 10 μM of (A) atorvastatin, (B) cerivastatin and (C) fluvastatin incubated at 5 and 10 minutes of incubation. Students t-test applied *P<0.05, **P<0.01, ***P<0.005 and ****P<0.0001

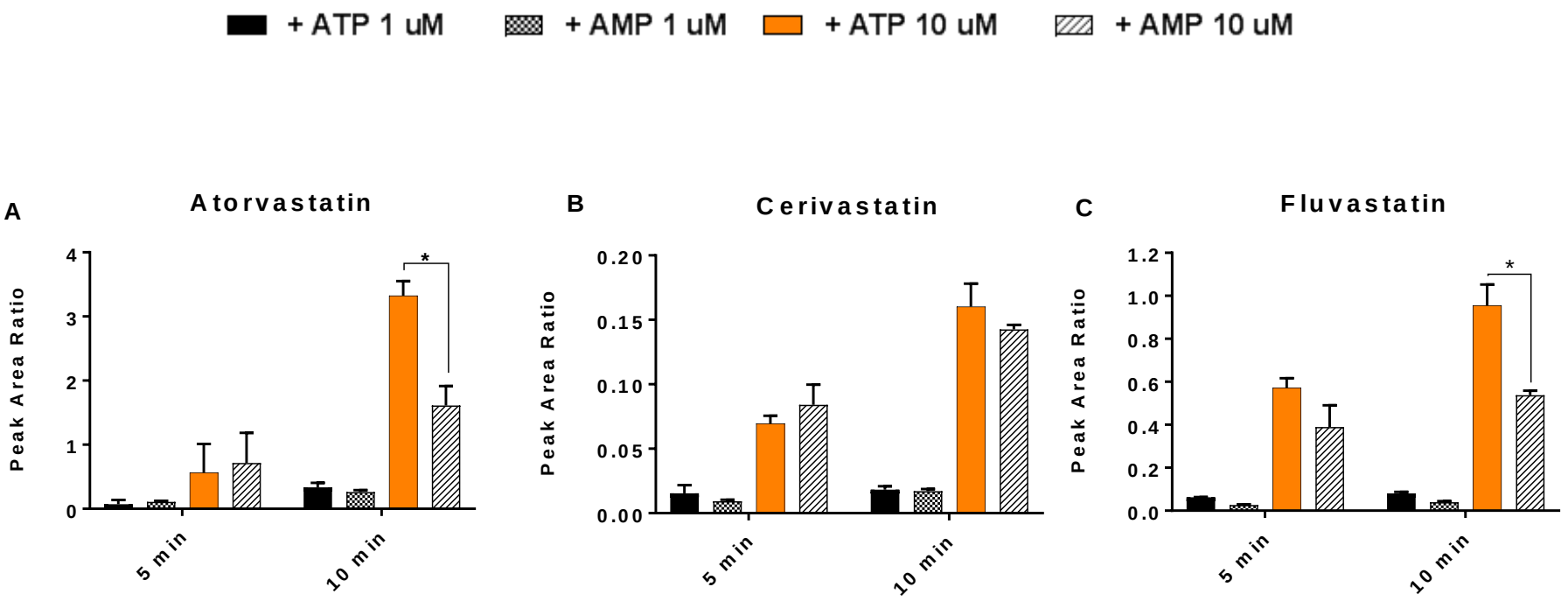

Appendix 16b.: Uptake of Statins on human MRP4 vesicles with 1 or 10 μM of (D)lovastatin, (E)pitavastatin, and (F) pravastatin at 5 and 20 minutes incubation. Students t-test applied *P<0.05, **P<0.01, ***P<0.005 and ****P<0.0001

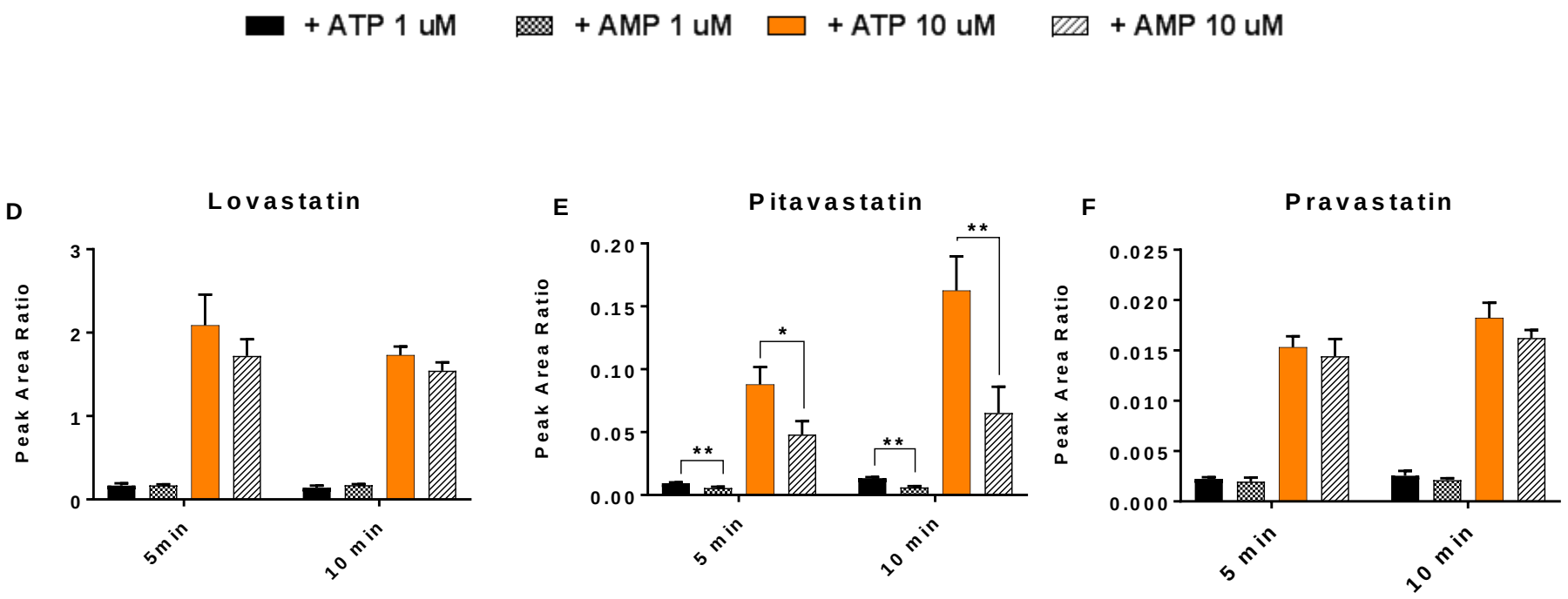

Appendix 16c. Uptake of Statins on human MRP4 vesicles with 1 or 10 µM (G) rosuvastatin, (H) Simvastatin at 5 and 10 minutes of incubations and (I) Positive control $E_2$17βg at 10 µM with 10 minutes of incubation. Students t-test applied *P<0.05, **P<0.01, ***P<0.005 and ****P<0.0001

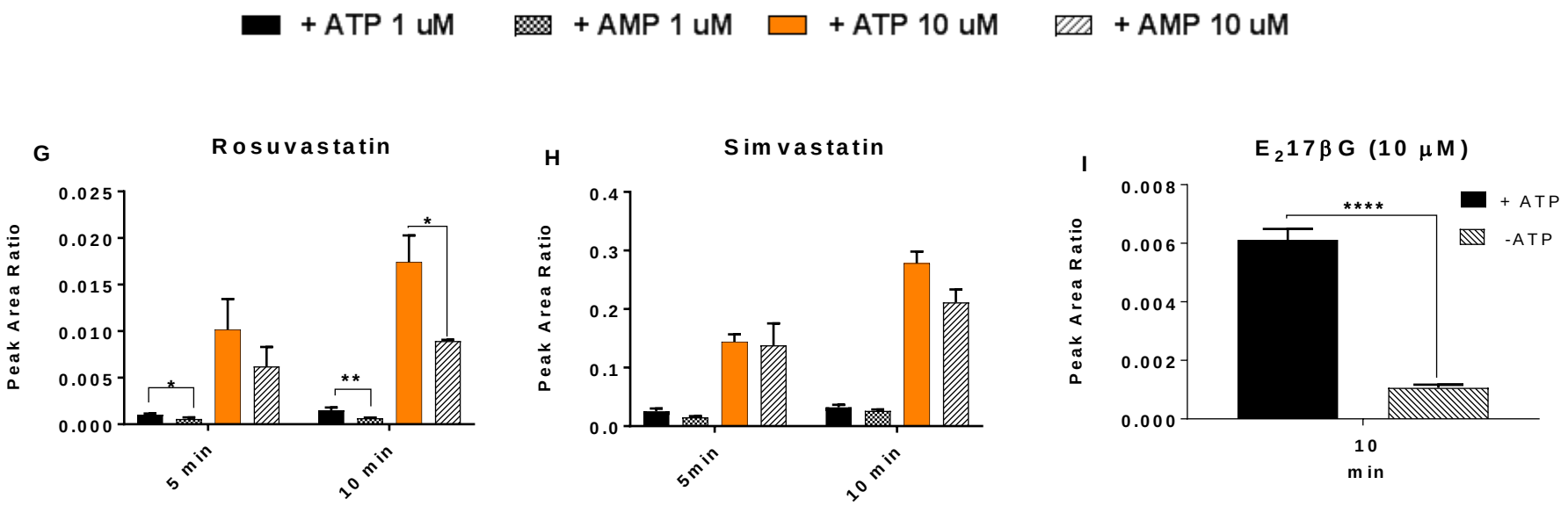

Appendix 17. Determination of kinetic parameters (A) Vmax from time course from uptake of 1µM Pravastatin on human MRP3 (B) Individual plots of concentration dependent uptake of pravastatin at 2.5 min on human MRP3 (C) Mean Plot of concentration dependent uptake of pravastatin at 2.5 min on human MRP3

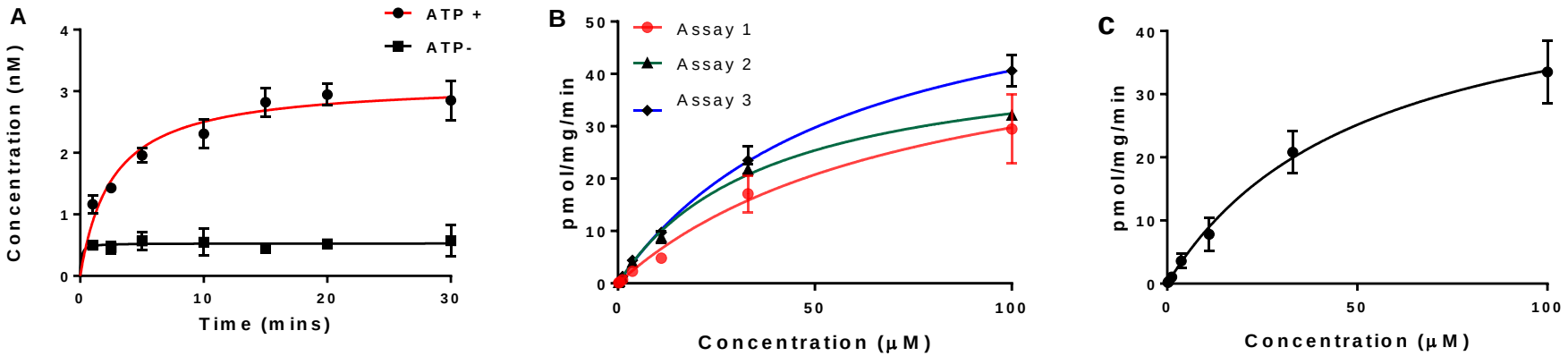

Appendix 18a Inhibition of 5 μM CDCF uptake into Human MRP2 vesicles by A) atorvastatin, (B) cerivastatin and (C) fluvastatin

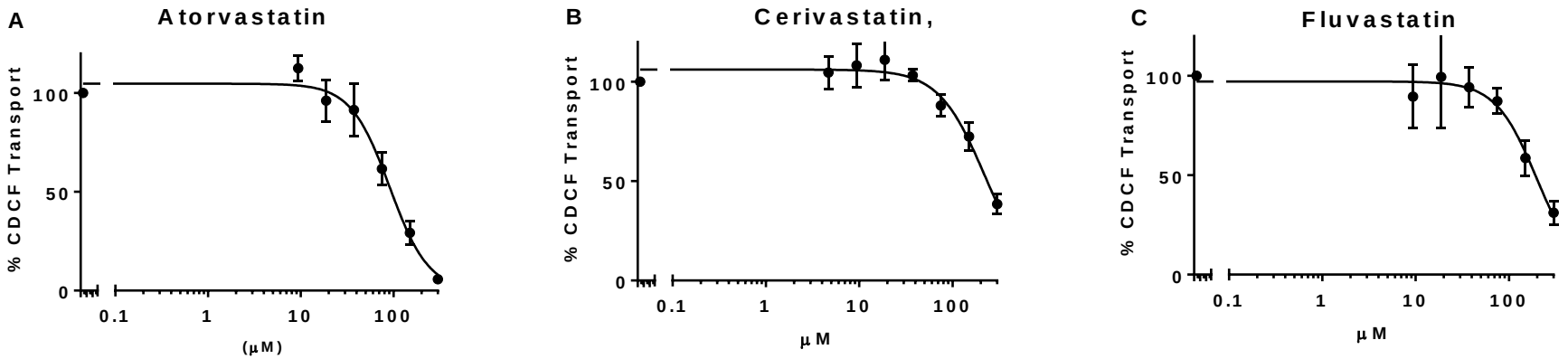

Appendix 18b. Inhibition of 5 μM CDCF uptake into Human MRP2 vesicles by (D)lovastatin, (E)pitavastatin and (F) pravastatin.

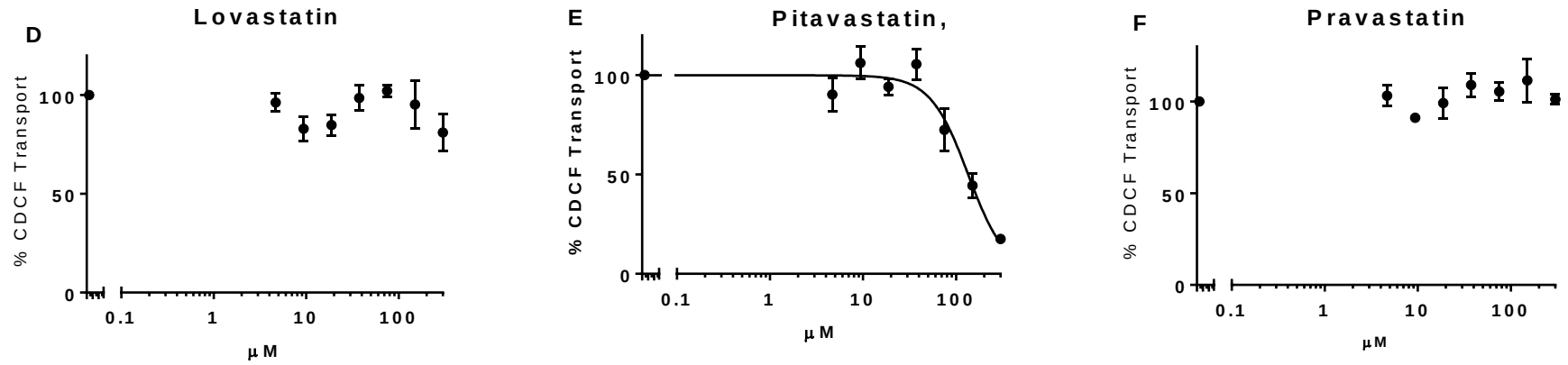

Appendix 18c. Inhibition of 5 µM CDCF uptake into Human MRP2 vesicles by (G)rosuvastatin, (H)Simvastatin, (I) Benzbromarone

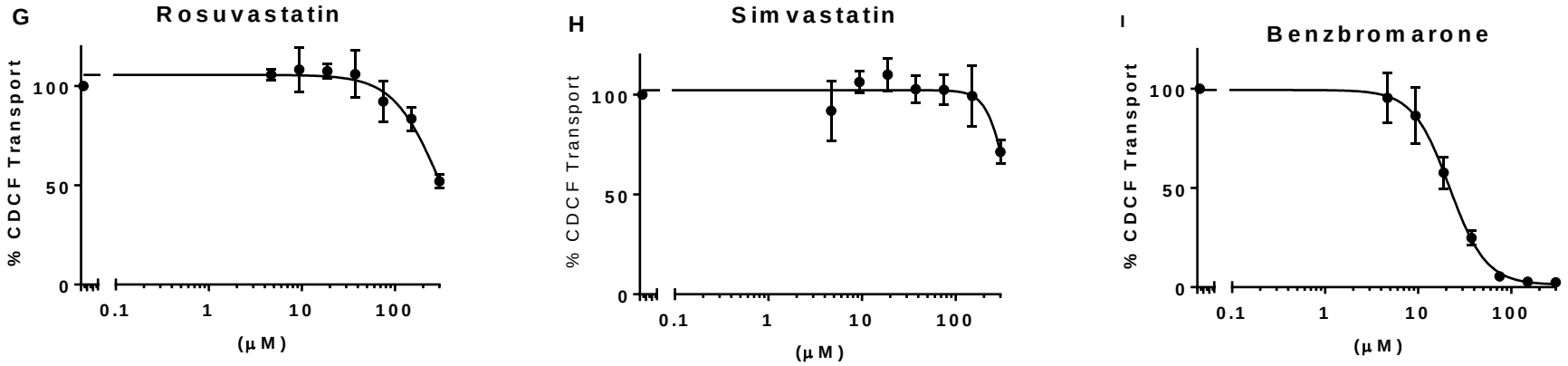

Appendix 19a. Inhibition of 5 μM CDCF uptake into Human MRP3 vesicles by A.1) atorvastatin A.2) repeat of atorvastatin, (B) cerivastatin and (C)fluvastatin,

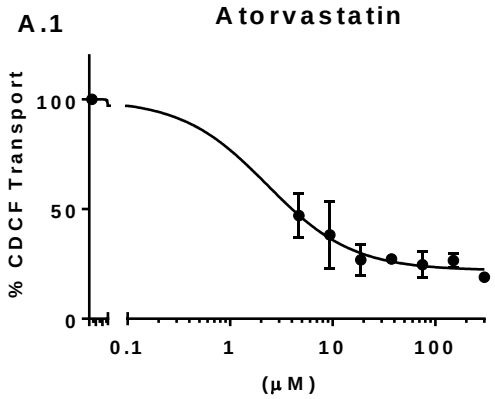

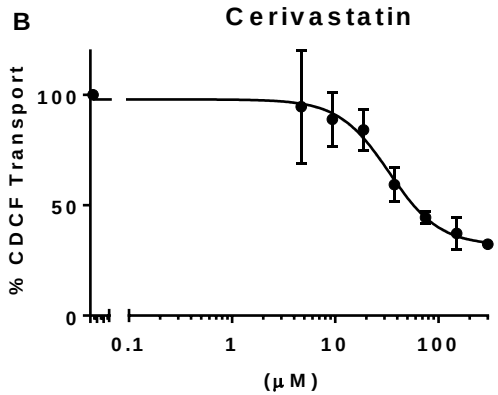

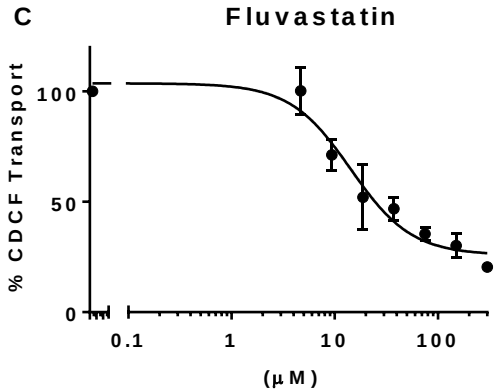

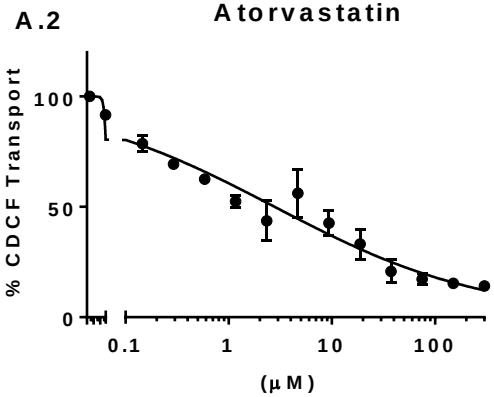

Appendix 19b. Inhibition of 5 μM CDCF uptake into Human MRP3 vesicles by (D)lovastatin, (E) pitavastatin and (F) pravastatin

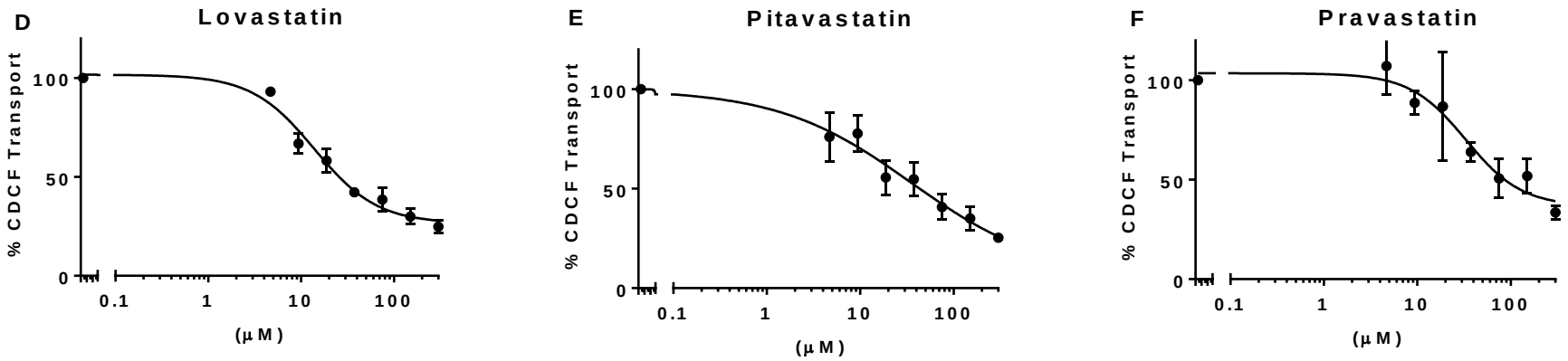

Appendix 19c. Inhibition of 5 μM CDCF uptake into Human MRP4 vesicles by (G)rosuvastatin, (H) simvastatin, (I) benzbromarone

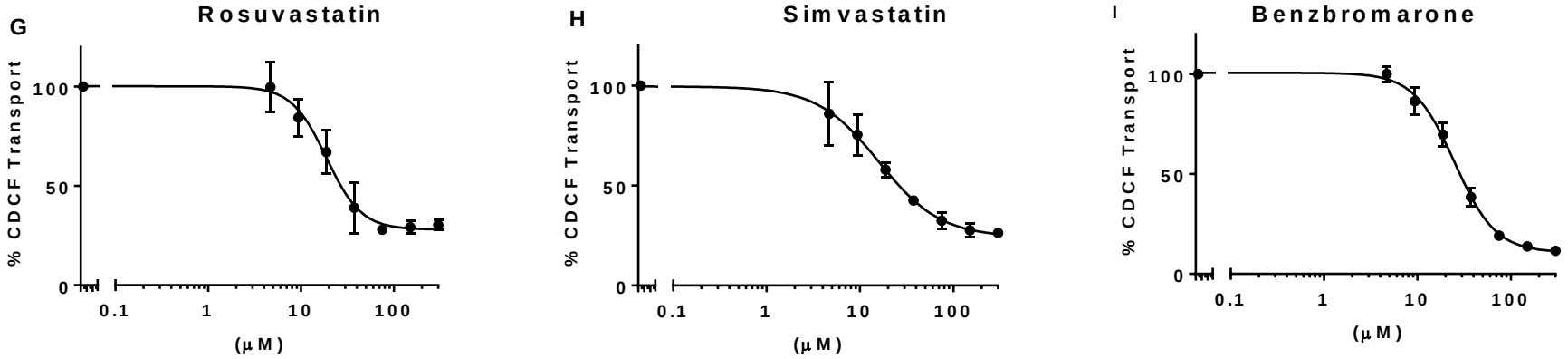

Appendix 20a. Inhibition of 10 μM $E_2$17βg uptake into Human MRP4 vesicles by A) atorvastatin, (B) cerivastatin and (C) fluvastatin

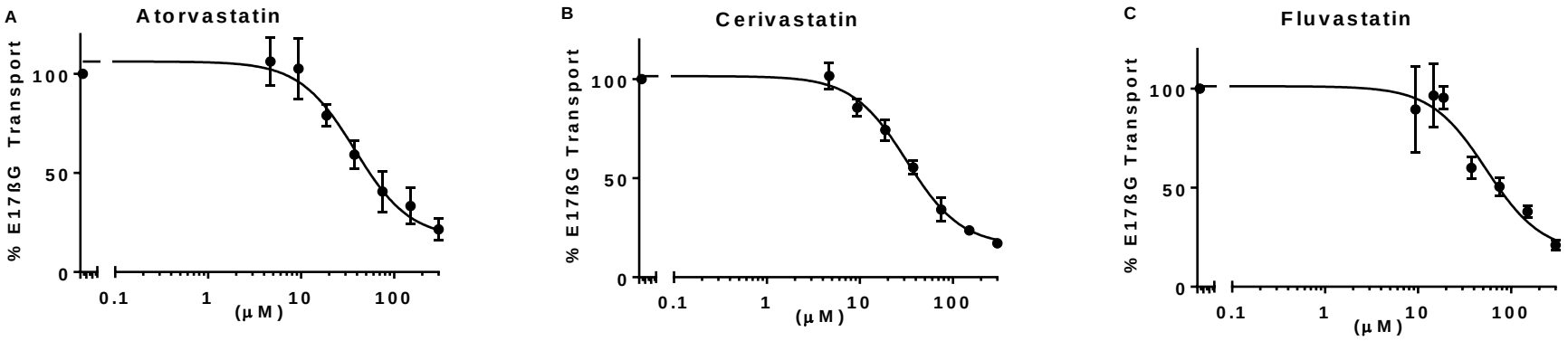

Appendix 20b. Inhibition of 10 μM $E_2$17βg uptake into Human MRP4 vesicles by (D)lovastatin, (E) pitavastatin and (F) pravastatin

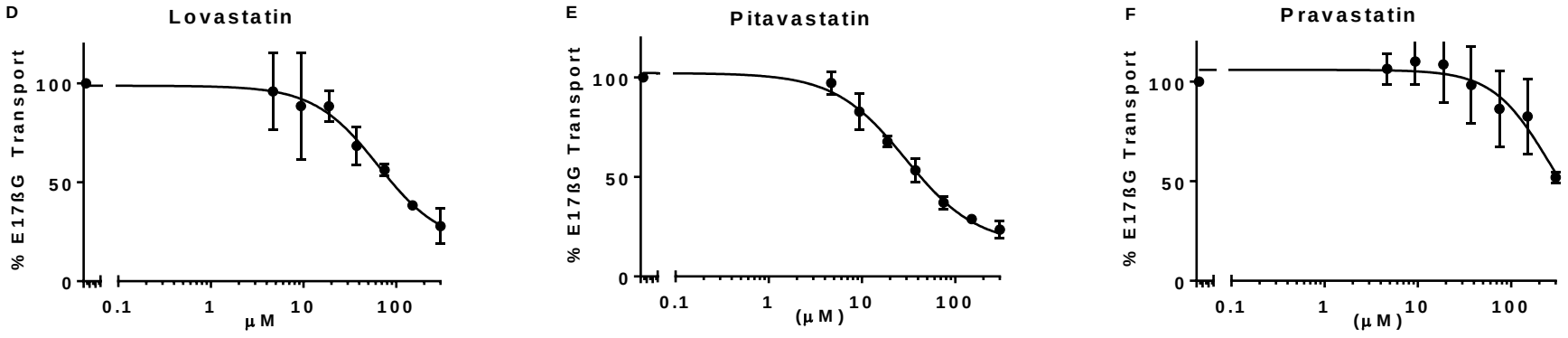

Appendix 20c. Inhibition of 10 μM $E_2$17βg uptake into Human MRP4 vesicles by (G)rosuvastatin, (H)Simvastatin, (I) MK571

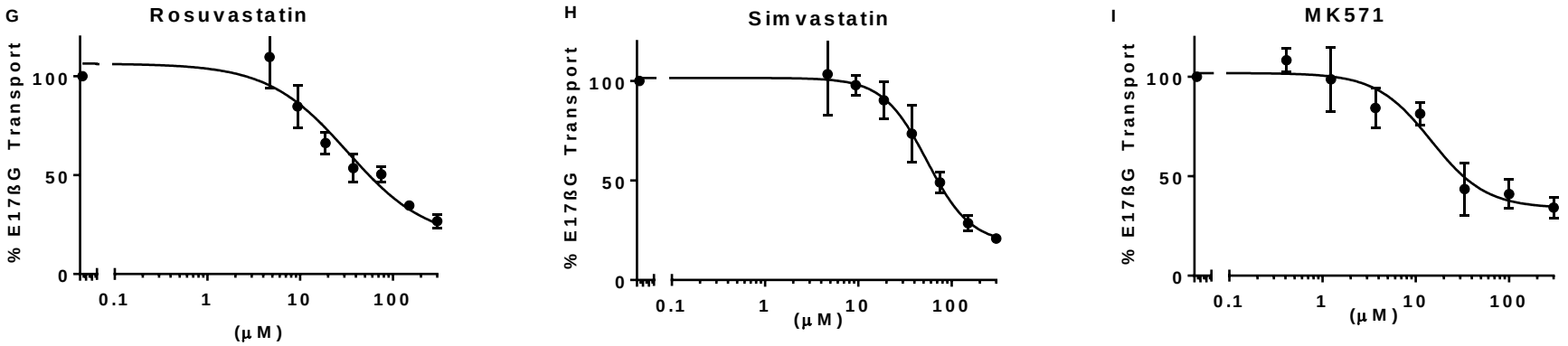

6 References

1. WHO. *The Top 10 Causes of Death*. Global Health Estimates 2016 2018 24May2018 [cited 2018 08October2018]; Available from: http://www.who.int/en/news-room/fact-sheets/detail/the-top-10-causes-of-death.
2. Berliner, J.A., et al., *Atherosclerosis: Basic Mechanisms.* Oxidation, Inflammation, and Genetics, 1995. **91**(9): p. 2488-2496.
3. Khera, A.V., *Cholesterol efflux capacity, high-density lipoprotein function, and atherosclerosis.* New England Journal of Medicine, 2011. **364**(2).
4. Rader, D.J., et al., *The role of reverse cholesterol transport in animals and humans and relationship to atherosclerosis.* Journal of Lipid Research, 2009. **50**(Supplement): p. S189-S194.
5. Minder, C.M., et al., *Evidence-based use of statins for primary prevention of cardiovascular disease.* The American journal of medicine, 2012. **125**(5): p. 440-446.
6. Minder, C.M., R.S. Blumenthal, and M.J. Blaha, *Statins for primary prevention of cardiovascular disease: the benefits outweigh the risks.* Current Opinion in Cardiology, 2013. **28**(5): p. 554-560.
7. O'Keeffe, A.G., I. Nazareth, and I. Petersen, *Time trends in the prescription of statins for the primary prevention of cardiovascular disease in the United Kingdom: a cohort study using The Health Improvement Network primary care data.* Clinical Epidemiology, 2016. **8**: p. 123-132.
8. McFarland, A.J., et al., *Molecular mechanisms underlying the effects of statins in the central nervous system.* Int J Mol Sci, 2014. **15**(11): p. 20607-37.
9. McKenney, J.M., *Pharmacologic characteristics of statins.* Clinical Cardiology, 2003. **26**(S3): p. 32-38.
10. Statista. *Leading chemical drugs dispensed in England in 2017, by items (in millions)*. 2018 [cited 2018 March2018]; Available from: https://www.statista.com/statistics/378445/prescription-cost-analysis-top-twenty-chemicals-by-items-in-england/.
11. Hawkes, N., *NICE guidelines could put 12 million UK adults on statins.* BMJ, 2017. **358**.
12. Rabar, S., et al., *Lipid modification and cardiovascular risk assessment for the primary and secondary prevention of cardiovascular disease: summary of updated NICE guidance.* BMJ: British Medical Journal (Online), 2014. **349**.
13. Chatzizisis, Y.S., *Risk factors and drug interactions predisposing to statin-induced myopathy.* Drug Safety, 2010. **33**(3).
14. Chapman, M.J.M.J., *Mechanisms of statin-induced myopathy: a role for the ubiquitin-proteasome pathway?* Arteriosclerosis, Thrombosis and Vascular Biology, 2005. **25**(12): p. 2441-4.
15. Graham, D.J., et al., *Incidence of hospitalized rhabdomyolysis in patients treated with lipid-lowering drugs.* JAMA, 2004. **292**(21): p. 2585-2590.
16. Staffa, J.A., J. Chang, and L. Green, *Cerivastatin and reports of fatal rhabdomyolysis.* New England Journal of Medicine, 2002. **346**(7): p. 539-540.
17. Ezad, S., H. Cheema, and N. Collins, *Statin-induced rhabdomyolysis: a complication of a commonly overlooked drug interaction.* Oxford medical case reports, 2018. **2018**(3): p. omx104-omx104.
18. Thompson, P.D., P.M. Clarkson, and R.S. Rosenson, *An Assessment of Statin Safety by Muscle Experts.* The American Journal of Cardiology, 2006. **97**(8, Supplement 1): p. S69-S76.
19. Knauer, M.J., et al., *Human skeletal muscle drug transporters determine local exposure and toxicity of statins.* Circ Res, 2010. **106**(2): p. 297-306.
20. Rodrigues, A.C., *Efflux and uptake transporters as determinants of statin response.* Expert Opinion on Drug Metabolism & Toxicology, 2010. **6**(5): p. 621-632.

21. Fujino, H., *Metabolic properties of the acid and lactone forms of HMG-CoA reductase inhibitors.* Xenobiotica, 2008. **34**(11-12): p. 11-12.
22. Neuvonen, P.J., M. Niemi, and J.T. Backman, *Drug interactions with lipid-lowering drugs: Mechanisms and clinical relevance.* Clinical Pharmacology & Therapeutics, 2006. **80**(6): p. 565-581.
23. Hirano, M., et al., *Contribution of OATP2 (OATP1B1) and OATP8 (OATP1B3) to the Hepatic Uptake of Pitavastatin in Humans.* Journal of Pharmacology and Experimental Therapeutics, 2004. **311**(1): p. 139-146.
24. Ieiri, I., et al., *SLCO1B1 (OATP1B1, an Uptake Transporter) and ABCG2 (BCRP, an Efflux Transporter) Variant Alleles and Pharmacokinetics of Pitavastatin in Healthy Volunteers.* Clinical Pharmacology & Therapeutics, 2007. **82**(5): p. 541-547.
25. Bi, Y.-a., et al., *Quantitative assessment of the contribution of sodium-dependent taurocholate co-transporting polypeptide (NTCP) to the hepatic uptake of rosuvastatin, pitavastatin and fluvastatin.* Biopharmaceutics & Drug Disposition, 2013. **34**(8): p. 452-461.
26. Lewis, D.F.V. and M. Dickins, *Substrate SARs in human P450s.* Drug Discovery Today, 2002. **7**(17): p. 918-925.
27. Fong, C.W., *Statins in therapy: Understanding their hydrophilicity, lipophilicity, binding to 3-hydroxy-3-methylglutaryl-CoA reductase, ability to cross the blood brain barrier and metabolic stability based on electrostatic molecular orbital studies.* European Journal of Medicinal Chemistry, 2014. **85**: p. 661-674.
28. Hamelin, B.A. and J. Turgeon, *Hydrophilicity/ lipophilicity: relevance for the pharmacology and clinical effects of HMG-CoA reductase inhibitors.* Trends in Pharmacological Sciences, 1998. **19**(1): p. 26-37.
29. Elsby, R., C. Hilgendorf, and K. Fenner, *Understanding the Critical Disposition Pathways of Statins to Assess Drug–Drug Interaction Risk During Drug Development: It's Not Just About OATP1B1.* Clinical Pharmacology & Therapeutics, 2012. **92**(5): p. 584-598.
30. Chen, C., et al., *DIFFERENTIAL INTERACTION OF 3-HYDROXY-3-METHYLGLUTARYL-COA REDUCTASE INHIBITORS WITH ABCB1, ABCC2, AND OATP1B1.* Drug Metabolism and Disposition, 2005. **33**(4): p. 537-546.
31. Neuvonen, P.J., J.T. Backman, and M. Niemi, *Pharmacokinetic Comparison of the Potential Over-the-Counter Statins Simvastatin, Lovastatin, Fluvastatin and Pravastatin.* Clinical Pharmacokinetics, 2008. **47**(7): p. 463-474.
32. Shitara, Y., *Clinical Importance of OATP1B1 and OATP1B3 in Drug–Drug Interactions.* Drug Metabolism and Pharmacokinetics, 2011. **26**(3): p. 220-227.
33. Pfeifer, N.D., et al., *Hepatic Basolateral Efflux Contributes Significantly to Rosuvastatin Disposition II: Characterization of Hepatic Elimination by Basolateral, Biliary, and Metabolic Clearance Pathways in Rat Isolated Perfused Liver.* Journal of Pharmacology and Experimental Therapeutics, 2013. **347**(3): p. 737-745.
34. Pfeifer, N.D., K. Yang, and K.L. Brouwer, *Hepatic basolateral efflux contributes significantly to rosuvastatin disposition I: characterization of basolateral versus biliary clearance using a novel protocol in sandwich-cultured hepatocytes.* Journal of Pharmacology and Experimental Therapeutics, 2013. **347**(3): p. 727-736.
35. Ellis, L.C.J., G.M. Hawksworth, and R.J. Weaver, *ATP-dependent transport of statins by human and rat MRP2/Mrp2.* Toxicology and Applied Pharmacology, 2013. **269**(2): p. 187-194.
36. Donner, M.G. and D. Keppler, *Up-regulation of basolateral multidrug resistance protein 3 (Mrp3) in cholestatic rat liver.* Hepatology, 2001. **34**(2): p. 351-359.
37. Assaraf, Y.G., *Molecular basis of antifolate resistance.* Cancer and Metastasis Reviews, 2007. **26**(1): p. 153-181.
38. Bakos, É., et al., *Interactions of the Human Multidrug Resistance Proteins MRP1 and MRP2 with Organic Anions.* Molecular Pharmacology, 2000. **57**(4): p. 760-768.

39. Zhou, S.-F., et al., *Substrates and Inhibitors of Human Multidrug Resistance Associated Proteins and the Implications in Drug Development.* Current Medicinal Chemistry, 2008. **15**(20): p. 1981-2039.
40. Bai, J., et al., *Multidrug resistance protein 4 (MRP4/ABCC4) mediates efflux of bimane-glutathione.* The International Journal of Biochemistry & Cell Biology, 2004. **36**(2): p. 247-257.
41. Chen, Z.-S., K. Lee, and G.D. Kruh, *Transport of Cyclic Nucleotides and Estradiol 17-β-d-Glucuronide by Multidrug Resistance Protein 4: RESISTANCE TO 6-MERCAPTOPURINE AND 6-THIOGUANINE.* Journal of Biological Chemistry, 2001. **276**(36): p. 33747-33754.
42. Zelcer, N., et al., *Steroid and bile acid conjugates are substrates of human multidrug-resistance protein (MRP) 4 (ATP-binding cassette C4).* Biochemical Journal, 2003. **371**(2): p. 361-367.
43. Kool, M., et al., *MRP3, an organic anion transporter able to transport anti-cancer drugs.* Proceedings of the National Academy of Sciences, 1999. **96**(12): p. 6914-6919.
44. Zeng, H., et al., *Transport of methotrexate (MTX) and folates by multidrug resistance protein (MRP) 3 and MRP1: effect of polyglutamylation on MTX transport.* Cancer research, 2001. **61**(19): p. 7225-7232.
45. Kruh, G.D. and M.G. Belinsky, *The MRP family of drug efflux pumps.* Oncogene, 2002. **22**: p. 7537.
46. Wilkens, S., *Structure and mechanism of ABC transporters.* F1000prime reports, 2015. **7**.
47. Jedlitschky, G., et al., *Transport of Glutathione, Glucuronate, and Sulfate Conjugates by the MRP Gene-encoded Conjugate Export Pump.* Cancer Research, 1996. **56**(5): p. 988-994.
48. Keitel, V., et al., *A common Dubin-Johnson syndrome mutation impairs protein maturation and transport activity of MRP2 (ABCC2).* American Journal of Physiology-Gastrointestinal and Liver Physiology, 2003. **284**(1): p. G165-G174.
49. Tsujii, H., et al., *Exon-intron organization of the human multidrug-resistance protein 2 (MRP2) gene mutated in Dubin–Johnson syndrome.* Gastroenterology, 1999. **117**(3): p. 653-660.
50. Chai, J., et al., *Elevated hepatic multidrug resistance-associated protein 3/ATP-binding cassette subfamily C 3 expression in human obstructive cholestasis is mediated through tumor necrosis factor alpha and c-Jun NH2-terminal kinase/stress-activated protein kinase–signaling pathway.* Hepatology, 2012. **55**(5): p. 1485-1494.
51. van Aubel, R.A., et al., *The MRP4/ABCC4 gene encodes a novel apical organic anion transporter in human kidney proximal tubules: putative efflux pump for urinary cAMP and cGMP.* Journal of the American Society of Nephrology, 2002. **13**(3): p. 595-603.
52. Denk, G.U., et al., *Multidrug resistance-associated protein 4 is up-regulated in liver but down-regulated in kidney in obstructive cholestasis in the rat.* Journal of hepatology, 2004. **40**(4): p. 585-591.
53. Weaver, R.J., *Assessment of drug-drug interactions: concepts and approaches.* Xenobiotica, 2001. **31**(8-9): p. 499-538.
54. Zhang, Z.-Y. and Y.N. Wong, *Enzyme kinetics for clinically relevant CYP inhibition.* Current drug metabolism, 2005. **6**(3): p. 241-257.
55. Patel, M., K.S. Taskar, and M.J. Zamek-Gliszczynski, *Importance of Hepatic Transporters in Clinical Disposition of Drugs and Their Metabolites.* The Journal of Clinical Pharmacology, 2016. **56**: p. S23-S39.
56. Chang, J.T., et al., *Rhabdomyolysis with HMG-CoA reductase inhibitors and gemfibrozil combination therapy.* Pharmacoepidemiology and Drug Safety, 2004. **13**(7): p. 417-426.
57. Swift*, B., N.D. Pfeifer*, and K.L. Brouwer, *Sandwich-cultured hepatocytes: an in vitro model to evaluate hepatobiliary transporter-based drug interactions and hepatotoxicity.* Drug metabolism reviews, 2010. **42**(3): p. 446-471.
58. Lew, V.L., et al., *Mechanism of spontaneous inside-out vesiculation of red cell membranes.* The Journal of Cell Biology, 1988. **106**(6): p. 1893-1901.

59. Steck, T.L., et al., *Inside-out red cell membrane vesicles: Preparation and puirification.* Science, 1970. **168**(3928): p. 255-257.
60. Kost, T.A., J.P. Condreay, and D.L. Jarvis, *Baculovirus as versatile vectors for protein expression in insect and mammalian cells.* Nature biotechnology, 2005. **23**(5): p. 567.
61. Telbisz, Á., et al., *Membrane cholesterol selectively modulates the activity of the human ABCG2 multidrug transporter.* Biochimica et Biophysica Acta (BBA) - Biomembranes, 2007. **1768**(11): p. 2698-2713.
62. Brouwer, K.L.R., et al., *In Vitro Methods to Support Transporter Evaluation in Drug Discovery and Development.* Clinical Pharmacology & Therapeutics, 2013. **94**(1): p. 95-112.
63. Kis, E., et al., *Effect of membrane cholesterol on BSEP/Bsep activity: species specificity studies for substrates and inhibitors.* Drug Metab Dispos, 2009. **37**(9): p. 1878-86.
64. Czuba, L.C., K.M. Hillgren, and P.W. Swaan, *Post-translational modifications of transporters.* Pharmacol Ther, 2018. **192**: p. 88-99.
65. Xu, D. and G. You, *Loops and layers of post-translational modifications of drug transporters.* Advanced Drug Delivery Reviews, 2017. **116**: p. 37-44.
66. Herédi-Szabó, K., E. Kis, and P. Krajcsi, *The Vesicular Transport Assay: Validated In Vitro Methods to Study Drug-Mediated Inhibition of Canalicular Efflux Transporters ABCB11/BSEP and ABCC2/MRP2*, in *Current Protocols in Toxicology*. 2001, John Wiley & Sons, Inc.
67. Krajcsi, P., *The Transporter Book*. 3rd ed. 2017: SOLVO Biotechnology, Budaors, Hungary.
68. Sarkadi, B., et al., *Expression of the human multidrug resistance cDNA in insect cells generates a high activity drug-stimulated membrane ATPase.* Journal of Biological Chemistry, 1992. **267**(7): p. 4854-4858.
69. Lanzetta, P.A., et al., *An improved assay for nanomole amounts of inorganic phosphate.* Analytical Biochemistry, 1979. **100**(1): p. 95-97.
70. *Fluorescence Detection Techniques*, in *Introduction to Fluorescence Sensing*, A.P. Demchenko, Editor. 2009, Springer Netherlands: Dordrecht. p. 65-118.
71. Eisenthal, R. and M.J. Danson, *Enzyme assays: a practical approach*. Vol. 257. 2002: Practical Approach (Paperback).
72. SOLVO, *VT-HTS-MRP4-HEK293-DHEAS/2.0 SB-MRP4 HEK293-VT: Determination of the Interaction of Drugs with the human MRP4 (ABCC4) transporter using the ^{3}H-DHEAS vesicular transport assay (for 96 well filter plates)*. Jan 2016.
73. GenoMembrane, *Vesicular Transport Assay Protocol For ABC Transporter Vesicle Product with RI-Labeled Subtrates.* VT assay for RI probe Ver.7.6.
74. Bodó, A., et al., *Differential modulation of the human liver conjugate transporters MRP2 and MRP3 by bile acids and organic anions.* Journal of Biological Chemistry, 2003. **278**(26): p. 23529-23537.
75. Herédi-Szabó, K., et al., *Potentiation of MRP2/Mrp2-Mediated Estradiol-17β-Glucuronide Transport by Drugs – A Concise Review.* Chemistry & Biodiversity, 2009. **6**(11): p. 1970-1974.
76. Na Li, B.B. *Application of a Fluorescent*

Substrate / Inside-Out Transporter

Vesicle Assay for Identifying

Inhibitors of MRP transport. 2010.
77. Akita, H., et al., *Transport Activity of Human MRP3 Expressed in Sf9 Cells: Comparative Studies with Rat MRP3.* Pharmaceutical Research, 2002. **19**(1): p. 34-41.
78. Russel, F.G.M., J.B. Koenderink, and R. Masereeuw, *Multidrug resistance protein 4 (MRP4/ABCC4): a versatile efflux transporter for drugs and signalling molecules.* Trends in Pharmacological Sciences, 2008. **29**(4): p. 200-207.
79. Hobbs, M., et al., *Understanding the interplay of drug transporters involved in the disposition of rosuvastatin in the isolated perfused rat liver using a physiologically-based pharmacokinetic model.* Xenobiotica, 2012. **42**(4): p. 327-338.

80. Abe, K., et al., *In Vitro Biliary Clearance of Angiotensin II Receptor Blockers and 3-Hydroxy-3-methylglutaryl-Coenzyme A Reductase Inhibitors in Sandwich-Cultured Rat Hepatocytes: Comparison with in Vivo Biliary Clearance.* Journal of Pharmacology and Experimental Therapeutics, 2008. **326**(3): p. 983-990.
81. Jemnitz, K., et al., *Biliary efflux transporters involved in the clearance of rosuvastatin in sandwich culture of primary rat hepatocytes.* Toxicology in Vitro, 2010. **24**(2): p. 605-610.
82. Kitamura, S., et al., *Involvement of multiple transporters in the hepatobiliary transport of rosuvastatin.* Drug Metabolism and Disposition, 2008. **36**(10): p. 2014-2023.
83. Lau, Y.Y., et al., *Multiple Transporters Affect the Disposition of Atorvastatin and Its Two Active Hydroxy Metabolites: Application of in Vitro and ex Situ Systems.* Journal of Pharmacology and Experimental Therapeutics, 2006. **316**(2): p. 762-771.
84. Kivistö, K.T., et al., *DISPOSITION OF ORAL AND INTRAVENOUS PRAVASTATIN IN MRP2-DEFICIENT TR[–] RATS.* Drug Metabolism and Disposition, 2005. **33**(11): p. 1593-1596.
85. Huang, L., Y. Wang, and S. Grimm, *ATP-dependent transport of rosuvastatin in membrane vesicles expressing breast cancer resistance protein.* Drug Metab Dispos, 2006. **34**(5): p. 738-42.
86. Martin, P.D., et al., *Metabolism, excretion, and pharmacokinetics of rosuvastatin in healthy adult male volunteers.* Clinical therapeutics, 2003. **25**(11): p. 2822-2835.
87. Singhvi, S.M., et al., *Disposition of pravastatin sodium, a tissue-selective HMG-CoA reductase inhibitor, in healthy subjects.* Br J Clin Pharmacol, 1990. **29**(2): p. 239-43.
88. Yamazaki, M., et al., *Biliary excretion of pravastatin in rats: contribution of the excretion pathway mediated by canalicular multispecific organic anion transporter (cMOAT).* Drug Metabolism and Disposition, 1997. **25**(10): p. 1123-1129.
89. Ho, R.H., et al., *Effect of drug transporter genotypes on pravastatin disposition in European- and African-American participants.* Pharmacogenetics and genomics, 2007. **17**(8): p. 647-656.
90. Kartenbeck, J., et al., *Absence of the canalicular isoform of the MRP gene–encoded conjugate export pump from the hepatocytes in Dubin-Johnson syndrome.* Hepatology, 1996. **23**(5): p. 1061-1066.
91. Niemi, M., *Transporter pharmacogenetics and statin toxicity.* Clinical Pharmacology and Therapeutics. **87**(1).
92. Fukumura, S., H. Takikawa, and M. Yamanaka, *Effects of organic anions and bile acid conjugates on biliary excretion of pravastatin in the rat.* Pharmaceutical research, 1998. **15**(1): p. 72-76.
93. König, J., et al., *Characterization of the human multidrug resistance protein isoform MRP3 localized to the basolateral hepatocyte membrane.* Hepatology, 1999. **29**(4): p. 1156-1163.
94. Inokuchi, A., et al., *Enhanced expression of the human multidrug resistance protein 3 by bile salt in human enterocytes: a transcriptional control of a plausible bile acid transporter.* Journal of Biological Chemistry, 2001.
95. Soroka, C.J., et al., *Cellular localization and up-regulation of multidrug resistance–associated protein 3 in hepatocytes and cholangiocytes during obstructive cholestasis in rat liver.* Hepatology, 2001. **33**(4): p. 783-791.
96. Borst, P., C. de Wolf, and K. van de Wetering, *Multidrug resistance-associated proteins 3, 4, and 5.* Pflügers Archiv - European Journal of Physiology, 2007. **453**(5): p. 661-673.
97. Gradhand, U., et al., *Variability in human hepatic MRP4 expression: influence of cholestasis and genotype.* The pharmacogenomics journal, 2008. **8**(1): p. 42.
98. Sugano, K., et al., *Coexistence of passive and carrier-mediated processes in drug transport.* Nature Reviews Drug Discovery, 2010. **9**: p. 597.
99. Sawant, R., *Rhabdomyolysis due to an uncommon interaction of ciprofloxacin with simvastatin.* Can J Clin Pharmacol, 2009. **16**(1): p. e78-e79.
100. Corsini, A. and S. Bellosta, *Drug–drug interaction with statins.* Expert Review of Clinical Pharmacology, 2008. **1**(1): p. 105-113.

101. Kyrklund, C., et al., *Gemfibrozil increases plasma pravastatin concentrations and reduces pravastatin renal clearance.* Clinical Pharmacology & Therapeutics, 2003. **73**(6): p. 538-544.
102. Lau, Y.Y., et al., *Effect of OATP1B transporter inhibition on the pharmacokinetics of atorvastatin in healthy volunteers.* Clinical Pharmacology and Therapeutics, 2007. **81**(2): p. 194-204.
103. Neuvonen, P.J., M. Niemi, and J.T. Backman, *Drug interactions with lipid-lowering drugs: mechanisms and clinical relevance.* Clinical Pharmacology & Therapeutics, 2006. **80**(6): p. 565-581.
104. Bogman, K., et al., *HMG-CoA reductase inhibitors and P-glycoprotein modulation.* British journal of pharmacology, 2001. **132**(6): p. 1183-1192.
105. Wang, E.-j., et al., *HMG-CoA Reductase Inhibitors (Statins) Characterized as Direct Inhibitors of P-Glycoprotein.* Pharmaceutical Research, 2001. **18**(6): p. 800-806.
106. Bruggisser, M., et al., *Liver damage in a patient treated with a vitamin K antagonist, a statin and an ACE inhibitor.* Praxis, 2010. **99**(21): p. 1259-1265.
107. Merli, M., et al., *Atorvastatin-induced prolonged cholestasis with bile duct damage.* Clinical drug investigation, 2010. **30**(3): p. 205-209.
108. Clarke, A. and P. Mills, *Atorvastatin associated liver disease.* Digestive and liver disease, 2006. **38**(10): p. 772-777.
109. Malinowski, J.M., *Atorvastatin: a hydroxymethylglutaryl-coenzyme A reductase inhibitor.* Am J Health Syst Pharm, 1998. **55**(21): p. 2253-67; quiz 2302-3.
110. Szabó, M., et al., *Statins alter the hepatobiliary transport of unconjugated and conjugated bilirubin in sandwich-cultured rat hepatocytes.* Toxicology in Vitro, 2014. **28**(6): p. 1136-1143.
111. Hirohashi, T., et al., *ATP-dependent transport of bile salts by rat multidrug resistance-associated protein 3 (Mrp3).* Journal of Biological Chemistry, 2000. **275**(4): p. 2905-2910.
112. Manautou, J.E., et al., *Altered disposition of acetaminophen in mice with a disruption of the Mrp3 gene.* Hepatology, 2005. **42**(5): p. 1091-1098.
113. Zelcer, N., et al., *Mice lacking multidrug resistance protein 3 show altered morphine pharmacokinetics and morphine-6-glucuronide antinociception.* Proceedings of the National Academy of Sciences, 2005. **102**(20): p. 7274-7279.
114. Chen, Z.-S., et al., *Analysis of Methotrexate and Folate Transport by Multidrug Resistance Protein 4 (ABCC4).* MRP4 Is a Component of the Methotrexate Efflux System, 2002. **62**(11): p. 3144-3150.